Characterization of the Cofactor Composition of *Escherichia coli* Biotin Synthase†

Michele Mader Cosper,‡ Guy N. L. Jameson,§ Heather L. Hernández,‡ Carsten Krebs,§,|| Boi Hanh Huynh,*,§ and Michael K. Johnson*,‡

Department of Chemistry and Center for Metalloenzyme Studies, University of Georgia, Athens, Georgia 30602, and Department of Physics, Emory University, Atlanta, Georgia 30322

Received September 15, 2003; Revised Manuscript Received November 21, 2003

ABSTRACT: The cofactor content of in vivo, as-isolated, and reconstituted forms of recombinant *Escherichia coli* biotin synthase (BioB) has been investigated using the combination of UV−visible absorption, resonance Raman, and Mössbauer spectroscopies along with parallel analytical and activity assays. In contrast to the recent report that *E. coli* BioB is a pyridoxal phosphate (PLP)-dependent enzyme with intrinsic cysteine desulfurase activity (Ollagnier-deChoudens, S., Mulliez, E., Hewitson, K. S., and Fontecave, M. (2002) *Biochemistry 41*, 9145−9152), no evidence for PLP binding or for PLP-induced cysteine desulfurase or biotin synthase activity was observed with any of the forms of BioB investigated in this work. The results confirm that BioB contains two distinct Fe−S cluster binding sites. One site accommodates a $[2Fe-2S]^{2+}$ cluster with partial noncysteinyl ligation that can only be reconstituted in vitro in the presence of O_2. The other site accommodates a $[4Fe-4S]^{2+,+}$ cluster that binds *S*-adenosylmethionine (SAM) at a unique Fe site of the $[4Fe-4S]^{2+}$ cluster and undergoes O_2-induced degradation via a distinct type of $[2Fe-2S]^{2+}$ cluster intermediate. In vivo Mössbauer studies show that recombinant BioB in anaerobically grown cells is expressed exclusively in an inactive form containing only the as-isolated $[2Fe-2S]^{2+}$ cluster and demonstrate that the $[2Fe-2S]^{2+}$ cluster is not a consequence of overexpressing the recombinant enzyme under aerobic growth conditions. Overall the results clarify the confusion in the literature concerning the Fe−S cluster composition and the in vitro reconstitution and O_2-induced cluster transformations that are possible for recombinant BioB. In addition, they provide a firm foundation for assessing cluster transformations that occur during turnover and the catalytic competence of the $[2Fe-2S]^{2+}$ cluster as the immediate S-donor for biotin biosynthesis.

Biotin synthase (BioB)[1] is a homodimeric Fe−S protein found in plants and microorganisms that plays a critical role in catalyzing the final step in the biosynthesis of biotin, namely, the activation of two C−H bonds for the stereospecific insertion of sulfur into dethiobiotin (DTB), see Scheme 1 (for recent reviews, see refs *1*−*4*). Spectroscopic and biochemical studies of *Escherichia coli* BioB (*5*−*7*) have provided overwhelming evidence that BioB is a member of the "radical-SAM" superfamily of Fe−S enzymes (*8*), which utilize a [4Fe−4S] cluster to generate a 5′-deoxyadenosyl radical via reductive cleavage of *S*-adenosyl-L-methionine (SAM). The 5′-deoxyadenosyl radical then abstracts a H atom from the C-9 position of DTB to yield a DTB radical (*9*). The subsequent steps and the nature of the immediate S donor are less well defined. Incorporation of deuterium at the C-6 position of DTB into the 5′-deoxyadenosine product and the requirement for at least two molecules of SAM for every molecule of biotin produced led Marquet to propose that ring closure involves an additional H-abstraction step involving a 5′-deoxyadenosyl radical generated from a second molecule of SAM (*9*). This model is further supported by the 2:1:1 SAM/DTB/BioB dimer binding stoichiometry that was recently reported by Jarrett and co-workers (*10*). In contrast, Fontecave and co-workers have reported a 1:1 stoichiometry of SAM/biotin using a pyridoxal 5′-phosphate (PLP)-dependent form of BioB (*11*). Likewise the nature of the immediate S donor is still controversial. While there is general agreement that cysteine is the ultimate source of S, both an additional [2Fe−2S] cluster (*12*, *13*) and a cysteine persulfide generated via cysteine desulfurase activity involving an indigenous protein-bound PLP (*14*) have been proposed as the immediate S donor to DTB on the basis of single turnover experiments.

Scheme 1

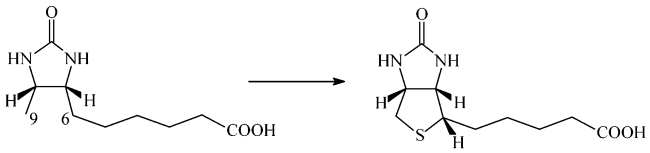

† This work was supported by grants from the National Institutes of Health (Grant GM62542 to M.K.J., Grant GM47295 to B.H.H. and a National Research Service Postdoctoral Fellowship to M.M.C, Grant DK59730).

* To whom correspondence should be addressed. M.K.J.: telephone, 706-542-9378; fax, 706-542-2353; e-mail, johnson@chem.uga.edu. B.H.H.: telephone, 404-727-4295; fax, 404-727-0873; e-mail, vhuynh@emory.edu.

‡ University of Georgia.

§ Emory University.

|| Current address: Department of Biochemistry and Molecular Biology, The Pennsylvania State University, University Park, PA 16802.

[1] Abbreviations: BioB, gene product of *bioB* commonly referred to as biotin synthase; SAM, *S*-adenosyl-L-methionine; DTB, dethiobiotin; DTT, dithiothreitol; DT, dithionite; PLP, pyridoxal 5′-phosphate.

10.1021/bi0356653 CCC: $27.50
Published on Web 01/30/2004

Although major progress has been made over the past decade, three major problems have impeded progress in characterizing the mechanism of *E. coli* BioB. The first is the inability to obtain more than one turnover, that is, 1 nmol of biotin per 1 nmol of BioB monomer, in a well-defined in vitro assay. However, the possibility that BioB is a reactant rather than an enzyme appears unlikely, since multiple turnovers have been reported using cell-free extracts containing overexpressed recombinant BioB both in *E. coli* (0.5 h^{-1}) (*15*) and in *Arabidopsis thaliana* (2.5−3 h^{-1}) (*16*). Rather the recent studies of Fontecave and co-workers using a PLP-dependent form of BioB indicate that the absence of multiple turnovers in vitro is a consequence of strong product inhibition by 5′-deoxyadenosine (*11*).

The second problem involves variability in the cofactor content. Although there is general agreement that aerobically isolated recombinant BioB contains only $[2Fe-2S]^{2+}$ clusters, the reported stoichiometries span the range 0.5−1.5 $[2Fe-2S]^{2+}$ clusters per monomer (*14*, *15*, *17*), and forms containing ∼2 $[2Fe-2S]^{2+}$ clusters per monomer have been claimed following incubation with $FeCl_3$ under argon (*17*). In accord with the initial discovery of reductive $[2Fe-2S]^{2+}$ to $[4Fe-4S]^{2+}$ cluster conversion in BioB (*5*), apo BioB reconstituted with $Fe(NH_4)_2(SO_4)_2$ or $FeCl_3$ and Na_2S under rigorously anaerobic conditions was subsequently found to contain approximately one $[4Fe-4S]^{2+,+}$ cluster per monomer (*18*). In contrast, anaerobic reconstitutions of as-isolated BioB using $FeCl_3$ and Na_2S in the presence of dithionite and 60% (v/v) ethylene glycol were reported to yield a form of BioB containing approximately two $[4Fe-4S]^{2+}$ clusters per monomer (*17*), and reconstitution of apo BioB using $FeCl_3$ and Na_2S under an argon atmosphere were found to contain approximately one $[2Fe-2S]^{2+}$ cluster per monomer (*19*). In addition, anaerobic reconstitution starting with as-isolated BioB in the absence of dithionite and ethylene glycol was found to result in a form of BioB containing approximately one $[2Fe-2S]^{2+}$ and one $[4Fe-4S]^{2+}$ per monomer that was capable of a single turnover in the absence of added iron and sulfide. This confusing picture has led to the hypothesis that BioB has two distinct cluster binding sites each of which is capable of binding either a $[2Fe-2S]^{2+}$ or $[4Fe-4S]^{2+}$ cluster with the catalytically relevant form corresponding to the form containing one $[2Fe-2S]^{2+}$ and one $[4Fe-4S]^{2+}$ cluster per monomer. BioB contains six conserved cysteine residues with the three in the rigorously conserved CxxxCxxC motif (Cys53, Cys57, and Cys60) involved in coordinating the redox active $[4Fe-4S]^{2+,+}$ cluster that is common to all members of the radical SAM family. The remaining three conserved cysteines (Cys97, Cys128, and Cys188) are good candidates for ligands of the [2Fe−2S] cluster. This hypothesis is supported by cysteine-to-alanine mutagenesis studies (*20*, *21*) and by resonance Raman studies, which indicate a $[2Fe-2S]^{2+}$ cluster with partial noncysteinyl ligation (*5*).

The debate over the cofactor content of the most active form of the enzyme has recently been reopened by the report that *E. coli* BioB is a PLP-dependent enzyme (*14*). PLP binding was reported for as-isolated BioB containing approximately 0.5 $[2Fe-2S]^{2+}$ cluster per monomer (0.3−0.4 PLP/monomer) and for anaerobically reconstituted [4Fe−4S] BioB (0.7−1.0 PLP/monomer). Moreover, the PLP-bound forms exhibited low levels of cysteine desulfurase activity that approximately correlated with the PLP content, and the PLP-bound [4Fe−4S] form of BioB was found to exhibit enhanced biotin synthase activity corresponding to a single turnover in the absence of added iron and sulfide. This led to the hypothesis that BioB has intrinsic PLP-dependent cysteine desulfurase activity, similar to that found in NifS and IscS (*22*, *23*), resulting in the formation of a cysteine persulfide on a conserved cysteine residue, which is subsequently attacked by the DTB radical (*14*). Loss of the PLP-dependent cysteine desulfurase activity in C97A and C128A BioB variants implicated Cys97 or Cys128 as the site for persulfide formation (*14*). Since the same conserved cysteines are proposed to be ligands to the [2Fe−2S] cluster, the current models for catalytic turnover involving a [2Fe−2S] cluster or a cysteine persulfide as the immediate S-donor appear to be mutually exclusive.

The third problem concerns the catalytic viability of recombinant forms of *E. coli* BioB. Whole cell Mössbauer studies of two BioB overexpressing strains of *E. coli* have recently been reported (*24*, *25*). For the strain used in this work (*E. coli* C41[DE3] pT7-7ecbioB-1), the results showed that recombinant BioB is predominantly, if not exclusively, expressed in an inactive form that contains only the $[2Fe-2S]^{2+}$ cluster (*24*). In contrast, both $[2Fe-2S]^{2+}$ and $[4Fe-4S]^{2+}$ clusters in a 3:1 ratio were found in the BioB expressed in the strain used by Marquet and co-workers (*E. coli* TK101 overexpressing BioB), indicating that a significant fraction of recombinant BioB contains a $[4Fe-4S]^{2+}$ prior to purification and therefore has the potential to be a catalytically competent form. Since both strains were grown aerobically, the partial or complete absence of the O_2-sensitive $[4Fe-4S]^{2+}$ cluster was tentatively attributed to O_2 exposure in the cell (*13*, *24*, *25*). Hence there is clearly a pressing need to characterize recombinant BioB from anaerobically grown cells to evaluate the possibility of deleterious effects of O_2 exposure during overexpression of BioB.

The objectives of this work were centered on resolving and addressing these three problematic areas of BioB research using the combination of absorption, resonance Raman, Mössbauer, and activity studies. Specifically, the objectives were to clarify the Fe−S cluster and PLP composition and activity of as-isolated and reconstituted forms of *E. coli* BioB, to investigate the effects of SAM and O_2 on the properties of individual Fe−S clusters in purified forms of BioB, and to establish the cofactor composition of recombinant BioB in anaerobically grown cells. The results support the existence of distinct $[4Fe-4S]^{2+}$ and $[2Fe-2S]^{2+}$ cluster binding sites in each BioB monomer, provide evidence for SAM binding to the $[4Fe-4S]^{2+}$ clusters in both the [4Fe−4S] and [2Fe−2S]/[4Fe−4S] forms of BioB, show that the $[4Fe-4S]^{2+}$ is rapidly degraded by O_2 via a distinct $[2Fe-2S]^{2+}$ intermediate, demonstrate that the as-isolated $[2Fe-2S]^{2+}$ cluster can be reconstituted in apo BioB in the presence of O_2, establish that recombinant BioB in anaerobically grown cells is expressed in an inactive form containing only the as-isolated $[2Fe-2S]^{2+}$ cluster, and provide no evidence in support of the proposal that BioB binds PLP or exhibits PLP-dependent cysteine desulfurase activity. Overall the results establish the Fe−S cluster composition and transformations that can occur for various forms of BioB and set the stage for electron

paramagnetic resonance (EPR) and Mössbauer studies to evaluate the proposal that the [2Fe−2S] cluster in the [2Fe−2S]/[4Fe−4S] form of BioB is the immediate S donor for biotin biosynthesis. The latter studies are presented in the accompanying manuscript.

MATERIALS AND METHODS

Materials. Chemicals were purchased from Sigma-Aldrich or Fisher, unless otherwise stated. ^{57}Fe−enriched ferric ammonium citrate and $FeSO_4$ were prepared from ^{57}Fe metal (>95% isotopic enrichment) as previously described (*24*). Restriction enzymes were purchased from New England Biolabs, and oligonucleotides were ordered from Integrated DNA Technologies. DNA sequencing was carried out by the Molecular Genetics Facility at the University of Georgia. The plasmid pBioBF2 containing the *E. coli bioB* gene was generously supplied by Dr. Katherine Gibson (E. I. du Pont de Nemours and Company, Wilmington), the plasmid pEE1010 containing the gene encoding *E. coli* flavodoxin reductase was a kind gift from Dr. Peter Reichard (Karolinska Institute, Sweden), and the plasmid pBH402 overexpressing polyhistidine-tagged *E. coli* IscS was a generous gift from Dr. Eugene Muller (University of Delaware). The *E. coli* strain DH01 overexpressing *E. coli* flavodoxin was a kind gift from Dr. Rowena Matthews (University of Michigan). The overexpression strain, *E. coli* C41[DE3], was provided by Professor John E. Walker (Medical Research Council, Cambridge, U.K.). Anaerobic experiments were performed under Ar in a Vacuum Atmospheres glovebox at oxygen levels <5 ppm. Apo BioB was prepared as previously described (*18*) except that sodium dithionite was used as the reductant in place of photochemical reduction mediated by 5-deaza-7,8-dimethyl-10-methyl-isoalloxazine.

Construction of the E. coli bioB Expression Vector pT7-7ecbioB-1. The gene encoding BioB was amplified using PCR from pBioBF2 using the primers 5′-GGAATTC-*CATATG*GCTCACCGCC-3′ and 5′-ACAA*CTGCAG*TCAT-AATGCTGCCG-3′. The PCR product was digested with *Nde* I and *Pst* I and ligated into the appropriately digested vector pT7-7 (*26*) to yield pT7-7ecbioB-1.

Aerobic Overexpression of E. coli BioB. The *E. coli* C41-[DE3] pT7-7ecbioB-1 strain was cultivated at 37 °C in terrific broth containing 100 μg/mL carbenicillin, 40 μg/mL Fe in the form of ferric ammonium citrate, or 12 μg/mL ^{57}Fe in the form of ferric ammonium citrate. When the cultures reached an OD_{600} between 0.9 and 1.2, isopropyl-1-thio-β-D-galactopyranoside (IPTG, Alexis) was added to a final concentration of 1.0 mM, and the bacteria cultures were further cultivated at 29 °C for 20 h. The cells were harvested by centrifugation at 4650 × *g* for 5 min at 4 °C and stored at −80 °C until further use.

Anaerobic Overexpression of E. coli BioB. The *E. coli* BL21-gold[DE3] pT7-7ecbioB-1 or *E. coli* BL21-gold[DE3] pT7-7 (control) strains were cultivated at 37 °C under strictly anaerobic conditions in Spizizen's minimal medium (*27*) with 10 mM $NaNO_3$, 20 μM Fe in the form of ferric ammonium citrate, 0.1% (w/v) casein hydroxylate, 1.5 μM thiamine, and 100 μg/mL amplicillin. When the cultures reached an OD_{600} between 0.9 and 1.2, IPTG was added to a final concentration of 0.05 mM, and the bacteria cultures were further cultivated at 37 °C for 3 h and finally stored at 4 °C for 16 h. The cells were harvested by centrifugation at 4650 × *g* for 5 min at 4 °C and stored at −80 °C until further use.

Anaerobic and Aerobic Purification of E. coli BioB. Six grams of cell paste was thawed and resuspended in 50 mM Hepes buffer, pH 7.5 (buffer A), with 20 μg/mL chicken egg-white lysozyme, 5 μg/mL DNase I (Roche), and 5 μg/mL RNase A (Roche). Cells were broken by intermittent sonication, and the cell debris was removed by centrifugation at 39 700 × *g* for 1 h at 4 °C. The cell-free extract was applied to a Source Q (Pharmacia) column (26 mm × 10 cm) previously equilibrated with buffer A and eluted with a 0−100% gradient of 50 mM Hepes buffer, pH 7.5, containing 1.0 M NaCl (buffer B). The purest fractions, as judged by SDS−PAGE analysis, were pooled and brought to a final concentration of 0.6 M in ammonium sulfate. This solution was applied to a phenyl sepharose high performance (Pharmacia) column (26 mm × 15 cm) previously equilibrated with 50 mM Hepes buffer, pH 7.5, containing 0.6 M ammonium sulfate (buffer C) and eluted with a 0−100% gradient of buffer A. The purest fractions, as determined by the A_{453}/A_{280} ratio (>0.215), were pooled and dialyzed into buffer A over a YM30 membrane. *E. coli* C41[DE3] pT7-7ecbioB-1 and BL21-gold[DE3] pT7-7ecbioB-1 cells yielded 2.5 mg of BioB/g of cell paste and 4.0 mg of BioB/g of cell paste, respectively. The same procedures were used for anaerobic and aerobic purifications, except that for anaerobic purifications, all manipulations were performed in the glovebox and all solutions were degassed prior to use by repeated freeze−pump−thaw cycles under Ar or purging with Ar for 1 h.

Construction of Vector pMCecbbhis-10 for Expression of his_6-BioB. The gene encoding BioB was amplified using PCR from pT7-7ecbioB-1 using the primers 5′-ATGGCTCAC-CGCCCACG-3′ and 5′-TAATGCTGCCGCGTTGTAATAT-TCGTC-3′. Using the TOPO cloning technology (Invitrogen), we ligated the PCR product into pCRT7/NT-TOPO to yield pMCecbbhis-10.

Overexpression and Purification of His-Tagged E. coli BioB. The *E. coli* BL21-gold[DE3] pMCecbbhis-10 strain was cultivated at 37 °C in LB containing 100 μg/mL amplicillin and 40 μg/mL Fe in the form of ferric ammonium citrate. When the cultures reached an OD_{600} between 0.6 and 0.8, IPTG was added to a final concentration of 0.1 mM, and the bacteria cultures were cultivated further at 37 °C for 3−5 h. Finally, the bacteria cultures were stored at 4 °C for 16 h under an Ar atmosphere. The cells were harvested by centrifugation at 4650 × *g* for 5 min at 4 °C.

Eight grams of cell paste was thawed and resuspended in 30 mL of 100 mM Tris-HCl buffer, pH 8.0, containing 0.3 M NaCl and 5 mM imidazole (buffer D), with 20 μg/mL chicken egg-white lysozyme, 5 μg/mL DNase I (Roche), and 5 μg/mL RNase A (Roche). Cells were broken by intermittent sonication, and the cell debris was removed by centrifugation at 39 700 × *g* for 1 h at 4 °C. The cell-free extract was loaded onto a charged and equilibrated 5 mL Ni-chelating column (Pharmacia), and the his_6-BioB was eluted with 0−100% gradient of 100 mM Tris-HCl buffer, pH 8.0, containing 0.3 M NaCl and 0.5 M imidazole (buffer E). The purest fractions, as determined by SDS−PAGE analysis, were pooled and dialyzed into buffer A over a YM30 membrane. *E. coli* BL21-gold[DE3] pMCecbbhis-10 cells yielded 5.0 mg of BioB/g of cell paste.

Reconstitution of [4Fe−4S]$^{2+}$ Centers in BioB. [4Fe−4S] BioB was prepared under strictly anaerobic conditions according to a previously published procedure (*18*), with the exception of the following modifications. Following incubation of apo BioB (280 μM) in 10 mM DTT for 10 min, a 10-fold molar excess of $Fe^{II}(NH_4)_2(SO_4)_2$ was added, followed by the addition of a 10-fold molar excess of Na_2S. After 1 h, the reconstitution mixture was loaded onto a 5 mL HiTrap Q column previously equilibrated with buffer A and eluted with a 0−100% gradient of buffer B. The brown fractions were concentrated over a YM30 (Amicon) membrane.

[2Fe−2S]/[4Fe−4S] BioB was prepared under strictly anaerobic conditions using the method of Jarrett and co-workers (*12*), with the following modifications. Following incubation of as-isolated [2Fe−2S] BioB in 10 mM DTT for 10 min, a 10-fold molar excess of $FeCl_3$, ferric ammonium citrate, $Fe^{II}(NH_4)_2(SO_4)_2$, or a 1:1 mixture of $FeCl_3$ and $Fe^{II}(NH_4)_2(SO_4)_2$ was added, followed by the addition of a 10-fold molar excess of Na_2S. After 1 h, the reconstitution mixture was loaded onto a 5-mL HiTrap Q column previously equilibrated with buffer A and eluted with a 0−100% gradient of buffer B. The red-brown fractions were concentrated over a YM30 (Amicon) membrane.

Reconstitution with Pyridoxal Phosphate (PLP) and Measurement of Cysteine Desulfurase Activity. Samples of *E. coli* BioB and PLP-depleted IscS-his_6 were incubated with a 5-to-10-fold molar excess of PLP at room temperature for time periods between 1 and 24 h in the presence of 5 mM DTT. Excess PLP was removed using a G-25 (Pharmacia) desalting column (26 mm × 15 cm), and the protein was concentrated over a YM30 (Amicon) membrane. The cysteine desulfurase activity of *E. coli* [4Fe−4S]$^{2+}$ BioB was assessed by analyzing for L-alanine and sulfide after anaerobic incubation with 1× PLP, 5 mM DTT, and 500 μM L-cysteine for 2.5 h at room temperature. The cysteine desulfurase activity of IscS-his_6 was assessed in parallel experiments without added PLP. L-Alanine was quantified according to the published procedure (*28*) using L-alanine dehydrogenase, which was generously provided by Dr. Robert Phillips (University of Georgia), and sulfide was quantified as previously described (*22*, *29*).

Determination of Protein, Fe, and PLP Concentrations. Protein concentrations were determined by the *DC* protein assay (Bio-Rad), using BSA as a standard. All protein concentrations for wild-type (WT) BioB determined using the *DC* protein assay were multiplied by the correction factor of 1.1, which was assessed on the basis of quantitative amino acid analyses of parallel samples (Commonwealth Biotechnologies). Iron concentrations were determined colorimetrically using bathophenanthroline under reducing conditions, after digestion of the protein in 0.8% $KMnO_4$/0.2 M HCl (*30*), and by inductively coupled plasma atomic emission spectroscopy (University of Georgia Chemical Analysis Laboratory). These two methods agreed to within ±5% for all samples investigated. All sample concentrations and molar extinction coefficients are expressed per BioB monomer. The concentration of bound PLP in BioB samples was assessed on the basis of absorption and analytical studies of alkaline-denatured samples according to the published procedures (*31*).

Spectroscopic Characterization of Fe−S Centers in BioB. UV−visible absorption spectra were recorded under anaerobic conditions in screw top 1 mm cuvettes using a Shimadzu UV-3101PC spectrophotometer. Resonance Raman spectra were recorded using an Instruments SA Ramanor U1000 spectrometer fitted with a cooled RCA 31034 photomultiplier tube with a 90° scattering geometry. Spectra were recorded digitally using photon counting electronics, and improvements in signal-to-noise were achieved by signal-averaging multiple scans. Band positions were calibrated using the excitation frequency and are accurate to ±1 cm^{-1}. Lines from a Coherent Sabre 10-W argon ion laser and plasma lines were removed using a Pellin Broca Prism premonochromator. With the use of a custom-designed sample cell (*32*), samples under an Ar atmosphere were placed on the end of a coldfinger of an Air Products Displex model CSA-202E closed cycle refrigerator. This enables the samples to be cooled to 17 K, which facilitates improved spectral resolution and prevents laser-induced sample degradation. Scattering was collected from the surface of a frozen 10 μL droplet. The Mössbauer spectra were recorded using the previously described spectrometers (*33*). The zero velocity refers to the centroid of the room-temperature spectra of metallic iron foil. Analysis of the Mössbauer data was performed with the program WMOSS (WEB Research).

Assay of Biotin Synthase Activity. The BioB assay was performed under strictly anaerobic conditions in a glovebox according to the procedure used by Fontecave and co-workers (*14*), except that the assays were performed at 25 °C rather than 37 °C. The assays were performed in 100 mM Tris-HCl buffer, pH 8.0, with BioB (35 μM), KCl (50 mM), DTT (5 mM), L-cysteine (2 mM), SAM (200 μM), *E.* coli flavodoxin (20 μM), *E.coli* flavodoxin reductase (5 μM), NADPH (1 mM), and dethiobiotin (375 μM). In accord with the results of Jarrett and co-workers (*12*), the omission of L-cysteine did not affect the assay results presented herein. Assays were performed in the absence and presence of 35 μM PLP or 1 mM $Fe^{II}(NH_4)_2(SO_4)_2$. Biotin was assayed using *Lactobacillus plantarum* ATCC 8014 according to published procedures (*34*, *35*).

RESULTS

Fe−S Cluster Stoichiometry and Conversions. Three distinct and well-defined forms of recombinant *E. coli* BioB were characterized on the basis of Fe and protein determinations and UV−visible absorption, resonance Raman, and Mössbauer properties: [2Fe−2S] BioB, which corresponds to as-isolated BioB, [4Fe−4S] BioB, which corresponds to anaerobically reconstituted apo BioB, and [2Fe−2S]/[4Fe−4S] BioB, which corresponds to anaerobically reconstituted as-isolated BioB. The properties of each form are summarized in Table 1 and compared below with previously published results on the Fe−S cluster stoichiometry of *E. coli* BioB.

[2Fe−2S] BioB. Fourteen different preparations of as-isolated recombinant *E. coli* BioB were investigated: 12 purified aerobically from aerobically grown cells, one purified under rigorously anaerobic conditions from aerobically grown cells, and one purified under rigorously anaerobic conditions from anaerobically grown cells. In all cases, the results were in remarkably good agreement with analyti-

Table 1: Cluster Composition, Absorption Properties, Mössbauer Parameters, and Activity of [2Fe−2S], [4Fe−4S], and [2Fe−2S]/[4Fe−4S] Forms of *E. coli* BioB

	cluster composition		absorption properties		Mössbauer parameters (4.2 K)				activity, biotin/BioB monomer[a]		
					$[2Fe-2S]^{2+}$		$[4Fe-4S]^{2+}$				
form	[2Fe−2S]/ BioB	[4Fe−4S]/ BioB	ϵ, $mM^{-1}\,cm^{-1}$ (nm)	ratio (A_{nm}/A_{nm})	δ, mm/s	ΔE_Q, mm/s	δ, mm/s	ΔE_Q, mm/s	no addition	with Fe^{2+}	with PLP
[2Fe−2S]	0.85 ± 0.10		7.2 ± 0.8 (453)	0.21 ± 0.02 (A_{453}/A_{278})	0.29	0.53			0.03	0.80	0.06
[4Fe−4S]		1.00 ± 0.10	15.6 ± 1.6 (410)	0.30 ± 0.03 (A_{410}/A_{278})			0.45 0.44	1.28 1.03	0.11	0.30	0.12
[2Fe−2S]/[4Fe−4S]	0.72 ± 0.05[b] 0.75 ± 0.09[c]	0.72 ± 0.05[b] 0.66 ± 0.05[c]	17.1 ± 1.8 (410)	0.33 ± 0.03 (A_{410}/A_{278})	0.28	0.5	0.45 0.43	1.32 1.08	0.62	0.70	0.62

[a] Nanomoles of biotin produced after 24 h at 25 °C per nanomoles of BioB monomer (estimated error ±10%). The assay mixture is as described in the Materials and Methods section without any additional components with 10× Fe^{2+} added to the reaction mixture, and with 1× PLP added to the reaction mixture. [b] Values derived from absorption data together with Fe and protein determinations. [c] Values derived from Mössbauer data together with Fe and protein determinations.

cal data indicating 1.7 ± 0.2 Fe/monomer and absorption spectra and molar extinction coefficients characteristic of approximately one $[2Fe-2S]^{2+}$ cluster per monomer (ϵ_{453} = 7.2 ± 0.8 $mM^{-1}\,cm^{-1}$ with A_{453}/A_{278} = 0.21 ± 0.02), see Figure 1a and Table 1. Moreover, both the resonance Raman and Mössbauer spectra confirm the presence of a homogeneous $[2Fe-2S]^{2+}$ center as the sole Fe−containing chromophore, see Figures 1a and 2a, respectively. Identical resonance Raman spectra were observed for all types of as-isolated sample investigated in this work, including His-tagged samples (see below), and the spectrum is characteristic of a unique type of $[2Fe-2S]^{2+}$ cluster with partial noncysteinyl ligation (*5*). Tentative vibrational assignments have been made by analogy with well-characterized 2Fe ferredoxins (*5*). The 4.2-K Mössbauer spectrum of as-isolated BioB (Figure 2a) exhibits a quadrupole doublet with parameters, δ = 0.29 mm/s and ΔE_Q = 0.53 mm/s, that are indicative of a $[2Fe-2S]^{2+}$ cluster. It is, however, inconclusive whether there is partial noncysteinyl ligation. These data are very similar to those reported in the original characterization of aerobically purified recombinant *E. coli* BioB (*5*, *15*) and for samples of *E. coli* BioB purified by other groups (*25*, *36*).

In contrast, Jarrett and co-workers reported that as-isolated samples of His-tagged *E. coli* BioB contained 1.2−1.5 $[2Fe-2S]^{2+}$ clusters per monomer based on Fe, S^{2-}, and protein analyses and that the Fe stoichiometry increased to 3.7 ± 0.4 Fe/monomer, corresponding to approximately 2 $[2Fe-2S]^{2+}$ clusters per monomer, following incubation with $FeCl_3$ and removal of excess Fe via anaerobic gel filtration (*17*). The same incubation/repurification procedure used by Jarrett and co-workers resulted in no change in the absorption and resonance Raman characteristics or the Fe/protein ratios for the wild-type recombinant samples of *E. coli* BioB used in this work. The possibility that one $[2Fe-2S]^{2+}$ cluster is labile and is lost during the more extensive and time-consuming purification protocol that is required for the wild-type protein compared to the His-tagged protein was investigated by purifying and analyzing samples of N-terminal His-tagged *E. coli* BioB (his_6-BioB) under both aerobic and rigorously anaerobic conditions. These samples were purified using a single Ni-chelating column but were found to be deficient in $[2Fe-2S]^{2+}$ clusters compared to the wild-type preparations: 1.4 ± 0.2 Fe/monomer and A_{453}/A_{278} = 0.17 ± 0.02. Hence despite extensive analytical and spectroscopic studies of a wide variety of samples, we have failed to find any evidence in support of a stable form of

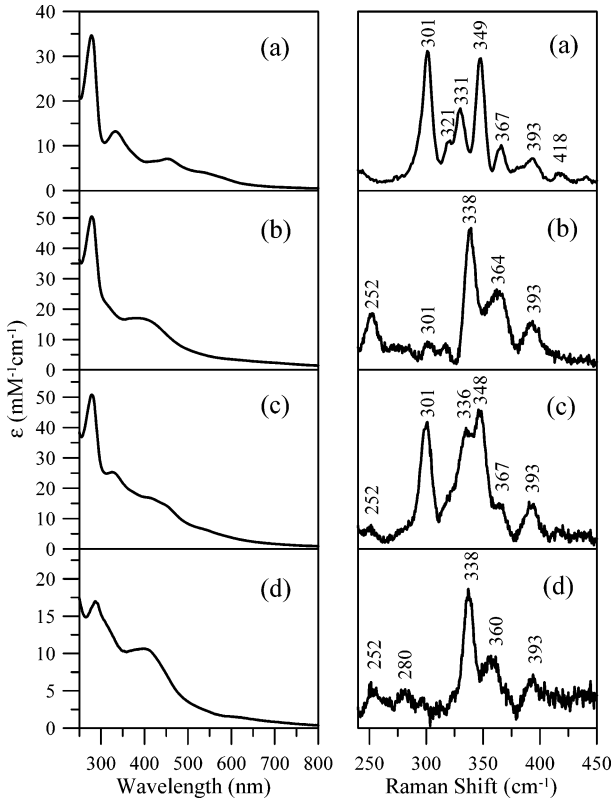

FIGURE 1: UV−visible absorption (left panel) and resonance Raman (right panel) spectra of *E. coli* BioB: (a) $[2Fe-2S]^{2+}$ BioB; (b) $[4Fe-4S]^{2+}$ BioB; (c) $[2Fe-2S]^{2+}/[4Fe-4S]^{2+}$ BioB. UV−visible absorption and resonance Raman difference spectra, c minus a, are shown in panel d. The UV−visible spectra were recorded in 1-mm cuvettes for samples of 290 μM $[2Fe-2S]^{2+}$ BioB, 170 μM $[4Fe-4S]^{2+}$ BioB, and 150 μM $[2Fe-2S]^{2+}/[4Fe-4S]^{2+}$ BioB in 50 mM Hepes buffer, pH 7.5. The resonance Raman spectra were recorded with 458-nm excitation, using samples that were ~3 mM in BioB frozen at 16 K with 210 mW laser power at the sample. Each scan involved photon counting for 1 s at 0.5 cm^{-1} increments with 8-cm^{-1} spectral resolution, and each spectrum is the sum of ~100 scans. A linear ramp fluorescence background has been subtracted from the resonance Raman spectra.

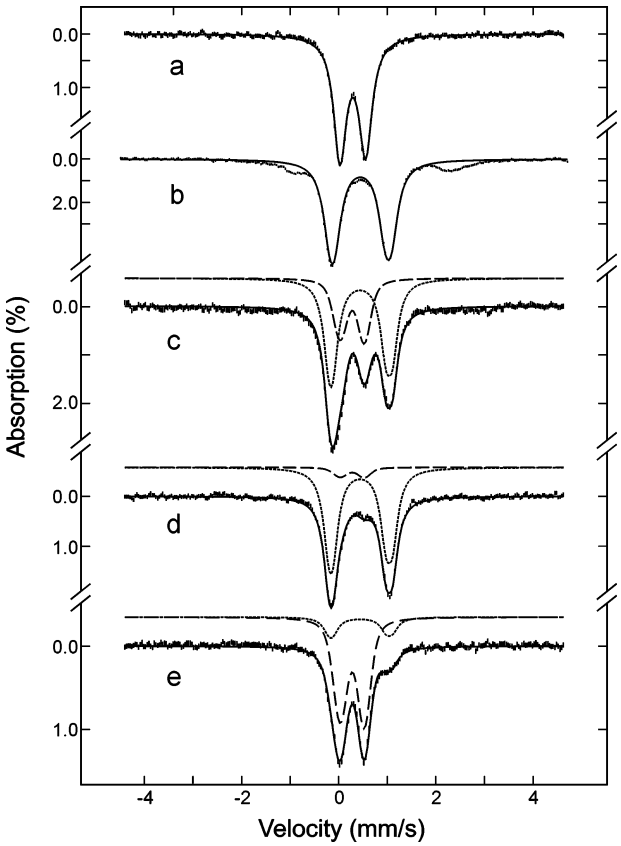

FIGURE 2: Mössbauer spectra (hatched marks) of [2Fe−2S], [4Fe−4S], and [2Fe−2S]/[4Fe−4S] *E. coli* BioB: (a) [^{57}Fe−2S] BioB, as-isolated from cells grown aerobically using ^{57}Fe in the form of ferric ammonium citrate as the sole source of Fe, 340 μM in BioB; (b) [4^{57}Fe−4S] BioB, prepared by anaerobic reconstitution of apo BioB using $^{57}Fe(NH_4)_2(SO_4)_2$, 130 μM in BioB; (c) [2^{57}Fe−2S]/[4^{57}Fe−4S] BioB, prepared by anaerobic reconstitution of as-isolated [2^{57}Fe−2S] BioB with $^{57}Fe(NH_4)_2(SO_4)_2$, 120 μM in BioB; (d) [2Fe−2S]/[4^{57}Fe−4S] BioB, prepared by anaerobic reconstitution of unlabeled as-isolated [2Fe−2S] BioB with $^{57}Fe(NH_4)_2(SO_4)_2$, 140 μM in BioB; (e) [2^{57}Fe−2S]/[4Fe−4S] BioB, prepared by anaerobic reconstitution of as-isolated [2^{57}Fe−2S] BioB with natural-abundance $Fe(NH_4)_2(SO_4)_2$ (2.2% ^{57}Fe), 140 μM in BioB. The solid lines shown in panels a and b are theoretical spectra of the $[2Fe-2S]^{2+}$ and $[4Fe-4S]^{2+}$ cluster, respectively, simulated with the parameters listed in Table 1. In panels c−e, the dashed and dotted lines are theoretical spectra of the $[2Fe-2S]^{2+}$ and $[4Fe-4S]^{2+}$ cluster, respectively, scaled to the absorption percentages listed in Table 1. The solid lines plotted over the data are summations of the two respective theoretical spectra. All samples contain 50 mM Hepes buffer, pH 7.5. The spectra were recorded at 4.2 K in a magnetic field of 50 mT oriented parallel to the γ beam.

as-isolated *E. coli* BioB containing more than one $[2Fe-2S]^{2+}$ cluster per monomer.

[4Fe−4S] BioB. Reconstitution of apo BioB under strictly anaerobic conditions using ferrous ammonium sulfate and sodium sulfide in the presence of DTT followed by anaerobic repurification using a HiTrap Q column resulted in a homogeneous form of BioB containing approximately one $[4Fe-4S]^{2+}$ cluster per monomer. Seven distinct reconstituted samples of recombinant wild-type apo BioB and two samples of apo his_6-BioB were investigated. The analytical data for all nine samples indicated 4.0 ± 0.4 Fe/monomer, and the absorption spectra were characteristic of a single $[4Fe-4S]^{2+}$ center per BioB monomer (ϵ_{410} = 15.6 ± 1.6 mM^{-1} cm^{-1} with A_{410}/A_{278} = 0.30 ± 0.03), see Figure 1b and Table 1.

Both the resonance Raman and Mössbauer spectra confirm the presence of a $[4Fe-4S]^{2+}$ center, see Figures 1b and 2b, respectively. Identical resonance Raman spectra were observed for all samples, including His-tagged samples, and the spectra are characteristic of a $[4Fe-4S]^{2+}$ cluster with the totally symmetric breathing mode at 338 cm^{-1} in a region of overlap between clusters with complete cysteinyl ligation and clusters with one noncysteinyl-ligated Fe (*5*, *7*). Tentative vibrational assignments have been made by analogy with those available for inorganic complexes containing $[4Fe-4S]^{2+}$ cores and well-characterized proteins with $[4Fe-4S]^{2+}$ clusters (*5*). With 458-nm excitation, the resonant enhancement of $[2Fe-2S]^{2+}$ centers is approximately 5-fold greater than that of $[4Fe-4S]^{2+}$ centers (*37*−*40*). Hence on the basis of the intensity of the weak band at 301 cm^{-1} that could be attributed to $[2Fe-2S]^{2+}$ clusters, we conclude that less than 5% of the BioB monomers in repurified reconstituted samples contain $[2Fe-2S]^{2+}$ clusters of the type seen in as-isolated samples of BioB. This conclusion was confirmed by Mössbauer studies.

The 4.2-K Mössbauer spectrum of an ^{57}Fe-reconstituted sample of apo BioB (Figure 2b) shows a major quadrupole doublet that is attributable to a $[4Fe-4S]^{2+}$ cluster and accounts for 90% of the ^{57}Fe absorption. This major doublet can be simulated as the sum of two overlapping equal intensity doublets, representing two valence-delocalized Fe^{II}-Fe^{III} pairs with parameters ($\delta(1)$ = 0.45 mm/s and $\Delta E_Q(1)$ = 1.28 mm/s and $\delta(2)$ = 0.44 mm/s and $\Delta E_Q(2)$ = 1.03 mm/s, see Table 1) that are typical for $[4Fe-4S]^{2+}$ clusters (*41*, *42*) and are similar to those reported for the $[4Fe-4S]^{2+}$ cluster in BioB (*7*, *18*). Spectra recorded in the presence of a strong magnetic field (data not shown) show that this major doublet originates from a diamagnetic species, consistent with a $[4Fe-4S]^{2+}$ cluster assignment. The remaining 10% ^{57}Fe absorption (small peaks at around −1 and 2 mm/s) is attributed to mononuclear ferrous impurities. The presence of $[2Fe-2S]^{2+}$ cluster is not detected.

Very similar results were reported by Fontecave and coworkers for anaerobically reconstituted and repurified samples of *E. coli* BioB (*18*). The only differences were that the reconstituted samples obtained by these workers contained a mixture of $[4Fe-4S]^{2+}$ and $[4Fe-4S]^{+}$ clusters, in addition to slightly larger amounts of mononuclear Fe^{2+} species (10−20% of ^{57}Fe absorption). Both differences are likely to be a consequence of anaerobic repurification using gel filtration rather than the HiTrap Q column used in this work. In contrast, reconstitution of wild-type apo BioB under semi-anaerobic conditions using ferric chloride and sodium sulfide in the presence of DTT has been reported to yield exclusively $[2Fe-2S]^{2+}$ clusters (0.85 $[2Fe-2S]^{2+}$ clusters per monomer) by Marquet and co-workers (*19*) and incubation of dithionite-treated as-isolated His-tagged BioB with ferric chloride and sodium sulfide in the presence of DTT and 60% (v/v) ethylene glycol was reported to lead to a derivative containing two $[4Fe-4S]^{2+}$ clusters per monomer by Jarrett and co-workers (*17*).

In an attempt to reconcile the conflicting reports concerning the products of cluster reconstitution procedures starting with apo BioB, we have duplicated the reconstitution procedures used by both the Marquet and Jarrett groups. In

accord with the results of Marquet and co-workers (*19*), analytical, absorption, and resonance Raman studies have confirmed that reconstitution with ferric chloride and sodium sulfide in the presence of DTT and oxygen does result in a $[2Fe-2S]^{2+}$-containing form of BioB almost indistinguishable from as-isolated BioB. This is best illustrated by the resonance Raman, which are compared in Figure 3, panels e and a, respectively. Hence the nature of the cluster reconstituted in BioB is critically dependent on the reconstitution conditions. However, using the reconstitution procedure reported by Jarrett and co-workers (*17*), we failed to find any evidence in support of a form of BioB containing two $[4Fe-4S]^{2+}$ clusters per monomer. Although the resulting samples exhibit similar absorption spectra and Fe analyses (∼8 Fe/momer BioB) to those reported by Jarrett and co-workers, the absorption spectrum has a pronounced shoulder centered at ∼600 nm that is characteristic of non-protein-associated soluble polymeric iron sulfides that exhibit broad absorption bands at 420 and 600 nm (*43*). This was confirmed by Mössbauer studies on samples reconstituted with ^{57}Fe, which revealed that approximately half of the Fe was present as $[4Fe-4S]^{2+}$ clusters with the remainder contributing to a broad underlying resonance indicative of polymeric iron sulfides (data not shown). Polymeric iron sulfides are invariably formed during in vitro reconstitution of Fe−S proteins and are often difficult to completely remove using gel filtration repurification protocol used by Jarrett and co-workers (*43*). The presence of this impurity therefore explains the anomalously high Fe determinations and molar extinction coefficients reported by Jarrett and co-workers. Moreover, we have found that this impurity can be removed by anaerobic repurification using a HiTrap Q column to yield a form of BioB containing a single $[4Fe-4S]^{2+}$ cluster on the basis of Fe determinations and absorption properties.

The $[4Fe-4S]^{2+}$ cluster that is assembled in BioB under anaerobic reconstitution conditions is known to be degraded by oxygen to yield a $[2Fe-2S]^{2+}$ cluster (*5*, *18*, *44*). However, the nature of the degradative process and the relationship of the resultant $[2Fe-2S]^{2+}$ cluster to the $[2Fe-2S]^{2+}$ cluster that is present in as-isolated BioB were unresolved questions prior to this study. Hence the time course of air-induced degradation of the $[4Fe-4S]^{2+}$ cluster in the presence of DTT was investigated using resonance Raman and Mössbauer spectroscopies. Resonance Raman proved to be particularly effective for investigating the nature of the $[2Fe-2S]^{2+}$ clusters generated during oxygen-induced degradation, see Figure 3. After 10 min of air exposure on the Raman probe, the resonance Raman bands associated with the $[4Fe-4S]^{2+}$ cluster (Figure 3b) have been replaced by a spectrum comprising broad bands centered at 292, 336, 366, and 395 cm^{-1} (Figure 3c). The spectrum is characteristic of a $[2Fe-2S]^{2+}$ cluster and is very similar to those reported for the $[2Fe-2S]^{2+}$ clusters generated via oxidative degradation of the $[4Fe-4S]^{2+}$ clusters in the nitrogenase Fe protein (*39*) and in other radical-SAM enzymes, for example, anaerobic ribonucleotide reductase activating enzyme (*45*), pyruvate formate-lyase activating enzyme (*46*), and the tRNA-methylthiotransferase, MiaB (*47*). However, mixing with aerobic buffer in a syringe for 1 h followed by aerobic centricon reconcentration resulted in the appearance of the characteristic resonance Raman spectrum associated with the $[2Fe-2S]^{2+}$ cluster found in as-isolated BioB (Figure 3d).

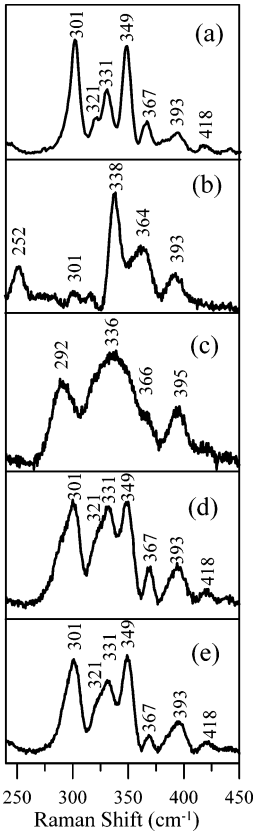

FIGURE 3: Resonance Raman spectra of [4Fe−4S] BioB during oxygen-induced cluster degradation and of aerobically reconstituted BioB: (a) as-isolated [2Fe−2S] BioB; (b) [4Fe−4S] BioB prepared by anaerobic reconstitution; (c) [4Fe−4S] BioB after exposure to air for 10 min on the Raman probe; (d) [4Fe−4S] BioB after exposure to air for 1 h; (e) [2Fe−2S] BioB prepared by reconstitution of apo BioB under aerobic conditions in the presence of DTT. The resonance Raman spectra were recorded with 458-nm excitation, using samples that were ∼3 mM in BioB frozen at 16 K with 210 mW laser power at the sample. Each scan involved photon counting for 1 s at 0.5 cm^{-1} increments with 8-cm^{-1} spectral resolution, and each spectrum is the sum of ∼100 scans. A linear ramp fluorescence background has been subtracted from the resonance Raman spectra.

The results indicate that oxygen-induced degradation of the $[4Fe-4S]^{2+}$ cluster proceeds via an unstable $[2Fe-2S]^{2+}$ cluster in a cluster conversion process that appears to be common to most members of the radical-SAM family. Furthermore, taken together with the results of aerobic reconstitution, see above and Figure 3e, the data indicate that this cluster degradation process is subsequently followed by aerobic reconstitution of the as-isolated $[2Fe-2S]^{2+}$ cluster on apo BioB using the ferric ion and sulfide that is generated by the cluster degradation process. Since the latter process is unique to BioB, the most likely explanation for the dramatic difference in the resonance Raman spectra of the $[2Fe-2S]^{2+}$ centers is that the as-isolated $[2Fe-2S]^{2+}$ cluster and the transient $[2Fe-2S]^{2+}$ cluster that results from oxygen-induced damage of the $[4Fe-4S]^{2+}$ cluster occupy distinct sites on BioB. Mössbauer studies confirmed rapid oxygen-induced degradation of the $[4Fe-4S]^{2+}$ cluster and subsequent formation of $[2Fe-2S]^{2+}$ clusters (data not shown). Unfortunately, Mössbauer spectroscopy does not have the required resolution to distinguish the two distinct types of $[2Fe-2S]^{2+}$ clusters that are observed in parallel resonance Raman studies.

[2Fe−2S]/[4Fe−4S] BioB: Convincing evidence for a form of *E. coli* BioB containing approximately one $[2Fe-2S]^{2+}$ and one $[4Fe-4S]^{2+}$ cluster per monomer has come from Fe and S analyses, absorption spectra, and Mössbauer studies of samples of as-isolated [2Fe−2S] BioB that were reconstituted under anaerobic conditions using ferric chloride and sodium sulfide in the presence of DTT (*17*, *48*). Using the same reconstitution procedure, we have used the combination of Fe analyses, coupled with UV/visible absorption, resonance Raman, and Mössbauer spectroscopy to confirm the existence of separate $[2Fe-2S]^{2+}$ and $[4Fe-4S]^{2+}$ cluster binding sites in BioB and to investigate perturbations in each of the clusters that are induced by the presence of the second cluster, see Figures 1 and 2 and Table 1. In accord with the results of Jarrett and co-workers (*17*), the absorption spectrum of anaerobically reconstituted as-isolated $[2Fe-2S]^{2+}$ BioB is readily understood in terms of approximately equal contributions from $[2Fe-2S]^{2+}$ and $[4Fe-4S]^{2+}$ chromophores, see Figure 1c. This is best illustrated by the reconstituted minus as-isolated difference spectrum, which has a broad shoulder at 410 nm that is characteristic of a $[4Fe-4S]^{2+}$ cluster. However, in contrast to the results of Jarrett and co-workers, which reported stoichiometric $[2Fe-2S]^{2+}$ and $[4Fe-4S]^{2+}$ clusters on the basis of analytical data that indicated 5.8 ± 0.3 Fe atoms and 6.2 ± 0.2 S^{2-} ions per monomer, analyses of the 11 distinct preparations investigated in this work indicated only 4.3 ± 0.3 Fe atoms per monomer. In addition, analyses of the absorption spectra using the extinction coefficients determined for $[4Fe-4S]^{2+}$ and $[2Fe-2S]^{2+}$ clusters in BioB, see above, consistently indicated 0.72 ± 0.10 $[4Fe-4S]^{2+}$ and $[2Fe-2S]^{2+}$ clusters per monomer, see Table 1. This discrepancy is likely to be a consequence of using a HiTrap-Q column for repurification of BioB in this work, rather than the gel filtration procedure used by Jarrett and co-workers. Indeed, subsequent Mössbauer studies of a sample repurified by gel filtration alone showed that 36% of the Fe was not associated with $[2Fe-2S]^{2+}$ or $[4Fe-4S]^{2+}$ clusters (*48*).

The vibrational properties of the clusters in [2Fe−2S]/[4Fe−4S] BioB were investigated using resonance Raman with 458-nm excitation, see Figure 1c. The spectrum is clearly dominated by the vibration modes of the as-isolated $[2Fe-2S]^{2+}$ cluster, compare spectra 1c with 1a. However, subtraction of the resonance Raman spectrum of as-isolated [2Fe−2S] BioB, see Figure 1d, results in a spectrum characteristic of a $[4Fe-4S]^{2+}$ cluster and very similar to that of the $[4Fe-4S]^{2+}$ cluster in [4Fe−4S] BioB, compare Figure 1, spectra b and d. The small shift in the asymmetric Fe−S(Cys) stretching mode of the $[4Fe-4S]^{2+}$ center (364 cm^{-1} in [4Fe−4S] BioB compared to 360 cm^{-1} in [2Fe−2S]/[4Fe−4S] BioB) may not be significant and may be a consequence of the subtraction procedure. Likewise, subtraction of the resonance Raman spectrum of [4Fe−4S] BioB to minimize the intensity of the 252-cm^{-1} band results in a spectrum very similar to that of the $[2Fe-2S]^{2+}$ cluster in as-isolated BioB (data not shown). Although the resonance Raman cannot provide an accurate assessment of the relative amounts of each type of cluster, the spectra support distinct binding sites for $[2Fe-2S]^{2+}$ and $[4Fe-4S]^{2+}$ clusters in BioB with the presence of the additional cluster having only minor effects on the environment of the original cluster.

The most conclusive evidence for distinct $[2Fe-2S]^{2+}$ and $[4Fe-4S]^{2+}$ binding sites in [2Fe−2S]/[4Fe−4S] BioB comes from Mössbauer studies. The Mössbauer spectra of four samples of ^{57}Fe-labeled as-isolated [2Fe−2S] BioB after anaerobic reconstitution using ^{57}Fe and repurification using a HiTrap-Q column (Figure 2c) indicate the presence of approximately equivalent amounts of $[2Fe-2S]^{2+}$ and $[4Fe-4S]^{2+}$ clusters ($[4Fe-4S]^{2+}/[2Fe-2S]^{2+}$ ratio = 0.9 ± 0.2). Moreover, the Mössbauer spectrum of a sample of unlabeled [2Fe−2S] BioB reconstituted with ^{57}Fe (Figure 2d) shows that the added Fe is assembled almost exclusively into $[4Fe-4S]^{2+}$ clusters (92% into $[4Fe-4S]^{2+}$ clusters and 8% into $[2Fe-2S]^{2+}$ clusters), while the spectrum of a sample of ^{57}Fe-labeled [2Fe−2S] BioB reconstituted with ^{56}Fe (Figure 2e) indicated that the indigenous Fe remains largely in the $[2Fe-2S]^{2+}$ form (82% $[2Fe-2S]^{2+}$ and 18% $[4Fe-4S]^{2+}$). In accord with the resonance Raman data, the Mössbauer parameters for the $[2Fe-2S]^{2+}$ and $[4Fe-4S]^{2+}$ clusters are not significantly perturbed by the presence of the second cluster, see Table 1. Hence the spectroscopic data point to distinct, well-defined sites for both the $[2Fe-2S]^{2+}$ and $[4Fe-4S]^{2+}$ clusters. The Mössbauer results are in excellent agreement with those reported by Jarrett and co-workers (*48*). The only significant difference lies in the absence of the mononuclear Fe^{II} species in our samples, and this appears to be a consequence of repurification using a HiTrap-Q column rather than gel filtration.

Exposure of [2Fe−2S]/[4Fe−4S] BioB to air for 1 h results in complete degradation of the $[4Fe-4S]^{2+}$ cluster as evidenced by absorption, resonance Raman, and Mössbauer studies. Moreover, as for [4Fe−4S] BioB, the degradation of the $[4Fe-4S]^{2+}$ cluster was found to proceed via a $[2Fe-2S]^{2+}$ cluster intermediate. This is best demonstrated by resonance Raman studies of air-exposed samples of [2Fe−2S]/[4Fe−4S] BioB, see Figure 4. After 10 min of air exposure, the Raman bands associated with the $[4Fe-4S]^{2+}$ cluster are completely lost (cf. Figures 4a and 1c) and subtraction of the resonance Raman spectrum of $[2Fe-2S]^{2+}$ cluster in as-isolated [2Fe−2S] BioB (Figure 4b) results in a spectrum (Figure 4c) that closely resembles the $[2Fe-2S]^{2+}$ cluster produced during O_2-induced degradation of the $[4Fe-4S]^{2+}$ cluster in [4Fe−4S] BioB (Figure 4d). Hence under these conditions it is possible, at least transiently, to obtain a form of BioB with two distinct types of $[2Fe-2S]^{2+}$ clusters bound in different sites.

SAM Binding to the $[4Fe-4S]^{2+}$ Cluster in [2Fe−2S]/[4Fe−4S] BioB. Previous resonance Raman and Mössbauer studies of BioB have provided strong evidence for SAM binding to the unique Fe site of the $[4Fe-4S]^{2+}$ cluster in [4Fe−4S] BioB (*7*). Hence we have used the same approach to investigate whether SAM binding to the $[4Fe-4S]^{2+}$ cluster is perturbed by the presence of the $[2Fe-2S]^{2+}$ cluster in [2Fe−2S]/[4Fe−4S] BioB. Addition of a 10-fold excess of SAM had no effect on the resonance Raman or Mössbauer properties of the $[2Fe-2S]^{2+}$ cluster in [2Fe−2S] BioB (the resonance Raman spectrum is shown in Figure 5b). In contrast, both the resonance Raman and Mössbauer studies of [2Fe−2S]/[4Fe−4S] BioB indicate that the SAM-induced changes in the $[4Fe-4S]^{2+}$ cluster that were observed with [4Fe−4S] BioB (*7*) are also observed in [2Fe−2S]/[4Fe−4S] BioB. In the case of resonance Raman, this is best illustrated by comparing the spectrum obtained for [4Fe−

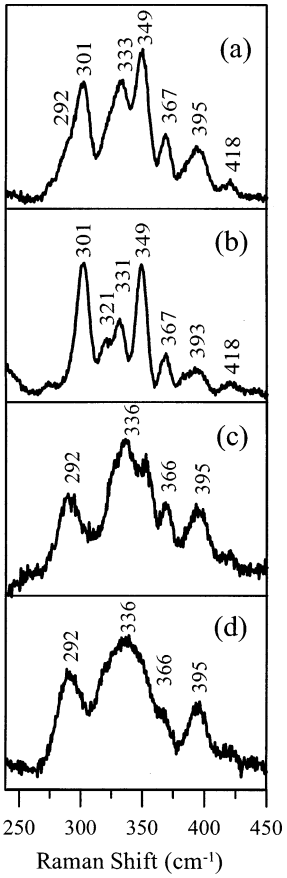

FIGURE 4: Resonance Raman spectra of [2Fe−2S]/[4Fe−4S] BioB after exposure to air for 10 min: (a) [2Fe−2S]/[4Fe−4S] BioB after exposure to air for 10 min on the Raman probe; (b) as-isolated [2Fe−2S] BioB; (c) difference spectrum a minus b. (d) [4Fe−4S] BioB after exposure to air for 10 min on the Raman probe. Measurement and sample conditions are as described in Figure 3.

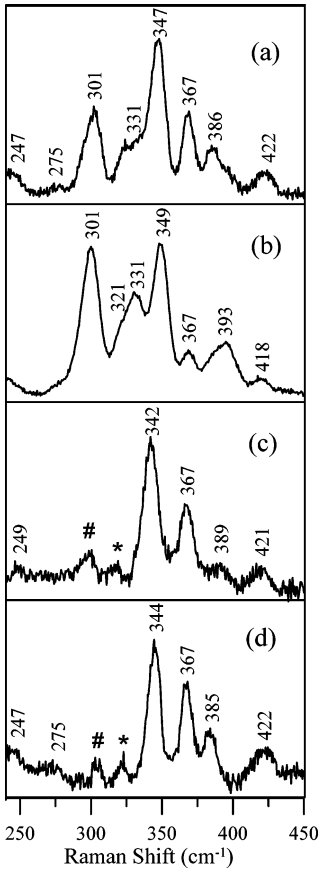

FIGURE 5: Resonance Raman spectra of *E. coli* BioB samples in the presence of a 10-fold stoichiometric excess of SAM: (a) [2Fe−2S]/[4Fe−4S] BioB; (b) [2Fe−2S] BioB; (c) [4Fe−4S] BioB. The difference spectrum corresponding to spectrum a minus spectrum b is shown in panel d. Samples were prepared in 50 mM Tris-HCl buffer, pH 8.5, with 1 mM DTT and 0.2 M NaCl. The resonance Raman spectra were recorded with 458-nm excitation, using samples that were ∼3 mM in BioB frozen at 16 K, with 210 mW laser power at the sample. Each scan involved photon counting for 1 s at 0.5 cm^{-1} increments with 8-cm^{-1} spectral resolution, and each spectrum is the sum of ∼100 scans. A linear ramp fluorescence background has been subtracted from the resonance Raman spectra. Bands resulting from residual $[2Fe-2S]^{2+}$ clusters and a lattice mode of ice are indicted by # and ∗, respectively.

4S] BioB + SAM (Figure 5c) with the [2Fe−2S]/[4Fe−4S] BioB + SAM minus [2Fe−2S] BioB + SAM difference spectrum (Figure 5d). The spectra are very similar, but quite distinct from the equivalent spectra obtained in the absence of SAM, see Figure 1, spectra b and d, respectively. The changes in the resonance Raman spectrum induced by SAM, in particular the increase in the frequency of the symmetric breathing mode of the Fe_4S_4 cube from 338 cm^{-1} in the absence of SAM to 342/344 cm^{-1} in the presence of SAM, are consistent with binding a bidentate noncysteinyl ligand at a unique Fe site of the $[4Fe-4S]^{2+}$ cluster (*7*). The effect of SAM binding on the Mössbauer spectrum of the $[4Fe-4S]^{2+}$ cluster in [2Fe−2S]/[4Fe−4S] BioB are most conveniently assessed using $[2^{56}Fe-2S]/[4^{57}Fe-4S]$ BioB. As shown in Figure 6, SAM binding induces marked changes in the Mössbauer spectrum of the $[4^{57}Fe-4S]^{2+}$ cluster in $[2^{56}Fe-2S]/[4^{57}Fe-4S]$ BioB, compare Figure 6, spectra a and b, and the changes are essentially identical to those previously reported for $[4^{57}Fe-4S]$ BioB, as judged by the near equivalence of the difference spectra for samples with and without SAM, compare Figure 6, spectra c and d. The SAM-induced changes in the Mössbauer spectrum have previously been analyzed in detail for $[4^{57}Fe-4S]$ BioB and attributed to an increase in coordination number or binding of a noncysteinyl ligand at a unique Fe site (*7*) or both. Hence the presence of the $[2Fe-2S]^{2+}$ does not alter the affinity or mode of binding of SAM to the $[4Fe-4S]^{2+}$ cluster in BioB.

Cluster Composition of Recombinant BioB in Anaerobically Grown E. coli cells. Our previous whole cell Mössbauer studies of recombinant BioB in aerobically grown cells revealed that the majority, if not all, of the overexpressed BioB was present inside the cells as an inactive form containing only $[2Fe-2S]^{2+}$ clusters (*24*). Hence the as-isolated $[2Fe-2S]^{2+}$ cluster was shown not to be an artifact of the purification procedure. However, because the as-isolated $[2Fe-2S]^{2+}$ cluster can be assembled in vitro only via an aerobic reconstitution procedure starting with apo BioB and the anaerobically reconstituted $[4Fe-4S]^{2+}$ cluster is rapidly degraded by exposure to oxygen, the whole cell studies raised the possibility that lack of the $[4Fe-4S]^{2+}$ cluster and the presence of the $[2Fe-2S]^{2+}$ might both be artifacts of overexpressing recombinant BioB under aerobic growth conditions (*24*). To test this hypothesis, we developed a BioB overproducing strain of *E. coli* suitable for anaerobic growth conditions and investigated the cluster content of cells grown on ^{57}Fe using whole cell Mössbauer spectroscopy. This strain was particularly effective for overexpression of

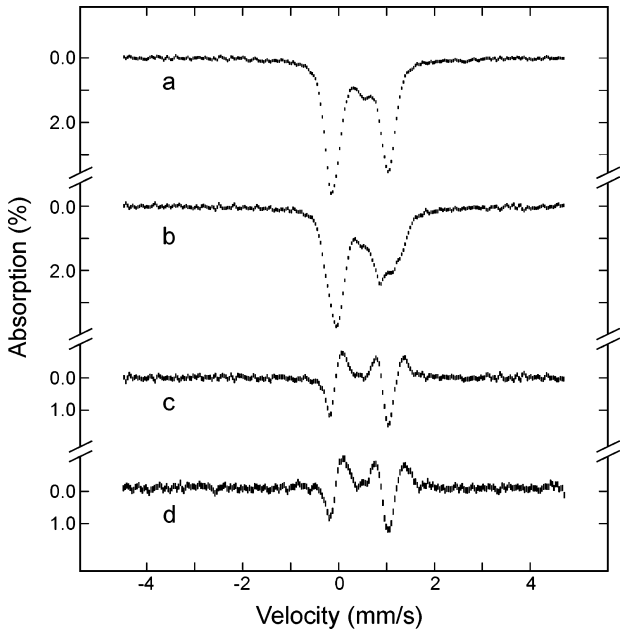

FIGURE 6: The effect of SAM on the Mössbauer spectrum of [2Fe−2S]/[4^{57}Fe−4S] BioB: (a) without SAM; (b) in the presence of a 10-fold stoichiometric excess of SAM. The spectra were recorded at 4.2 K in a magnetic field of 50 mT oriented parallel to the γ beam. The sample of [2Fe−2S]/[4^{57}Fe−4S] BioB was in 50 mM Tris-HCl buffer, pH 8.5, with 1 mM DTT and 0.2 M NaCl and was 275 μM in BioB. The difference spectrum corresponding to spectrum a minus spectrum b is shown in panel c. The previously published difference spectrum corresponding to [4^{57}Fe−4S] BioB minus [4^{57}Fe−4S] BioB plus 10× SAM is shown in panel d (*24*).

BioB and gel densitometry indicated that BioB accounted for approximately 20% of the total cellular protein.

The results of the whole cell Mössbauer study of recombinant BioB in anaerobically grown *E. coli* are shown in Figure 7. Control cells grown under identical conditions containing the same plasmid used for overexpressing BioB, but without the BioB insert, exhibited broad quadrupole doublets from ferric (Figure 7a, dashed line) and ferrous (Figure 7a, dotted line) components. In contrast, the dominant feature in the spectrum of cells with overexpressed BioB (Figure 7b) is a quadrupole doublet with parameters (δ = 0.29 mm/s and ΔE_Q = 0.53 mm/s) identical to those of the $[2Fe-2S]^{2+}$ cluster in as-isolated [2Fe−2S] BioB (Figure 6b). Moreover, removal of the ferrous and ferric contributions from the spectra obtained for whole cells and cell-free extract yields spectra (Figure 7, spectra c and d, respectively) that are indicative of $[2Fe-2S]^{2+}$ clusters, revealing that anaerobically overexpressed BioB contains only $[2Fe-2S]^{2+}$ clusters prior to purification. Hence recombinant BioB is shown to contain only $[2Fe-2S]^{2+}$ clusters in the overexpressing strains used in this work, irrespective of aerobic or anaerobic growth conditions.

Is BioB a PLP-Dependent Enzyme? Fontecave and coworkers have reported that BioB as purified contains 0.05 mol of PLP per mole of monomeric BioB and that incubation with a 5-fold excess of PLP in the presence 10 mM DTT, followed by extensive dialysis to remove excess PLP, results in incorporation of up to 0.4 mol of PLP per mole of [2Fe−2S] BioB and up to 1.0 mol of PLP per mole of [4Fe−4S] BioB (*14*). Moreover, PLP was found to induce significant cysteine desulfurase activity in [4Fe−4S] BioB and to enhance the biotin synthase activity of both the [2Fe−2S]

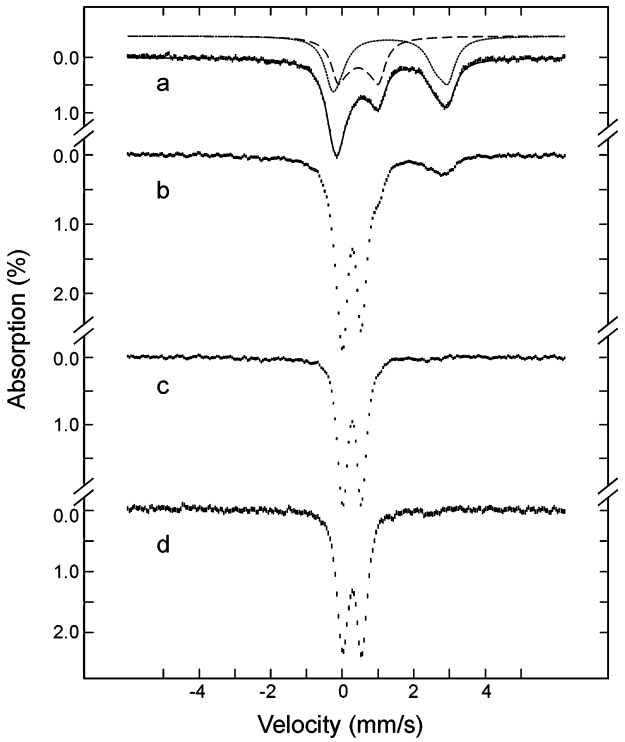

FIGURE 7: Mössbauer spectra (hatched marks) of anaerobically grown ^{57}Fe−enriched whole cells of *E. coli* with and without overexpression of BioB: (a) *E. coli* BL21-gold[DE3] pT7-7 control whole cells, which contain the same plasmid used for expression of BioB but without the *bioB* insert; (b) *E. coli* BL21-gold[DE3] pT7-7ecbioB-1 whole cells with overexpression of BioB. The spectra were recorded at 4.2 K in a magnetic field of 50 mT, oriented parallel to the γ beam. The dotted and dashed lines in panel a are theoretical simulations of the ferrous (55%) and ferric (45%) components, respectively. Each component is simulated using two equal-intensity quadrupole doublets with the following parameters: $\delta(1)$ = 1.34 mm/s, $\Delta E_Q(1)$ = 3.25 mm/s, $\Gamma(1)$ = 0.48 mm/s, $\delta(2)$ = 1.26 mm/s, $\Delta E_Q(2)$ = 2.74 mm/s, and $\Gamma(2)$ = 0.65 mm/s for the ferrous component and $\delta(1)$ = 0.45 mm/s, $\Delta E_Q(1)$ = 0.57 mm/s, $\Gamma(1)$ = 0.76 mm/s, $\delta(2)$ = 0.45 mm/s, $\Delta E_Q(2)$ = 1.15 mm/s, and $\Gamma(2)$ = 0.43 mm/s for the ferric component. The solid line in panel a is the addition of these two components. Removal of the contributions of the ferrous (17%) and ferric (24%) component from spectrum b yields the spectrum shown in panel c. The spectrum shown in panel d is the cell-free extract corresponding to the whole cell sample shown in spectrum b with the contributions of the ferrous (10%) and ferric (22%) components removed.

and [4Fe−4S] forms of BioB (*14*). As discussed below, we have been unable to confirm any of these results with the samples of *E. coli* BioB used in this work.

As-isolated [2Fe−2S] BioB and samples of [4Fe−4S] BioB reconstituted from apo BioB in the presence of a 10-fold stoichiometric excess of PLP, followed by gel-filtration to remove excess PLP, contained <0.01 mol of bound PLP per mole of monomeric BioB, as judged by absorption and analytical assessment of PLP in alkaline-denatured samples. Moreover, incubation of either [2Fe−2S] BioB or [4Fe−4S] BioB with a 5−10-fold excess of PLP in the presence of 5 mM DTT for time periods in the range 1−24 h provided no evidence of PLP binding as judged by absorption studies, see Figure 8. Following removal of excess PLP by gel filtration, the resulting absorption spectra exactly overlaid those of the starting material. The absence of bound PLP was confirmed by absorption and analytical studies of alkaline-denatured samples. In contrast, the same procedure

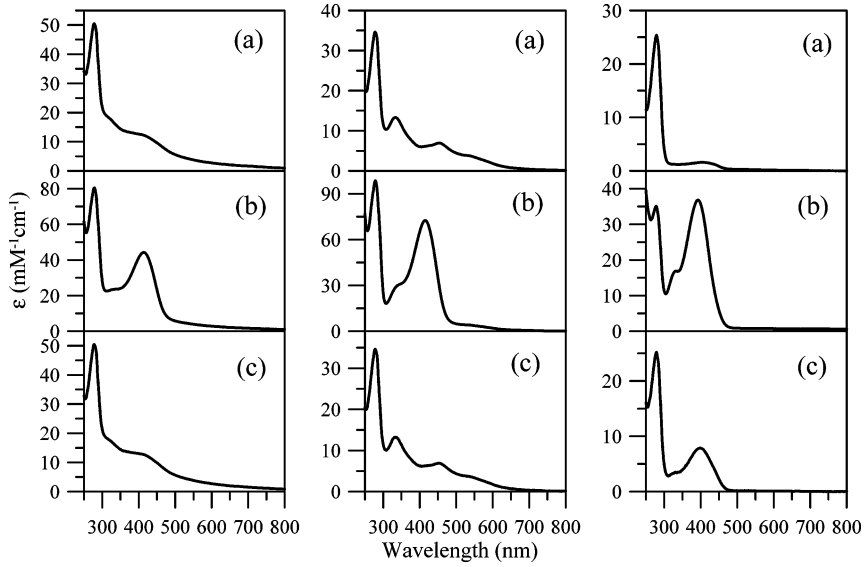

FIGURE 8: UV−visible absorption spectra of *E. coli* [4Fe−4S] BioB (left panel), *E. coli* [2Fe−2S] BioB (middle panel), and *E. coli* IscS-his$_6$ (right panel): (a) before the addition of PLP; (b) in the presence of a 5−10-fold molar excess of PLP; (c) after removal of excess PLP using a desalting column. The spectra were recorded in 1-mm cuvettes using 170 μM [2Fe−2S] BioB and 240 μM [4Fe−4S] BioB, both in 50 mM Hepes buffer, pH 7.5, with 5 mM DTT, and 350 μM IscS-his$_6$ in 50 mM potassium phosphate buffer, pH 7.5, with 5 mM $MgCl_2$, 100 mM KCl, and 0.1 mM EDTA.

Table 2: Assays of *E. coli* $[4Fe-4S]^{2+}$ BioB and His-Tagged IscS for Cysteine Desulfurase Activity[a]

$[4Fe-4S]^{2+}$ BioB				
[BioB], μM	[PLP], μM	Ala/BioB[b]	S^{2-}/BioB	Ala/S^{2-}
20	20	<0.25	4.4	<0.1
20	0	<0.25	4.1	<0.1
40	40	<0.13	4.1	<0.1
40	0	<0.13	3.6	<0.1
His-Tagged IscS				
[IscS], μM	[PLP], μM	Ala/IscS	S^{2-}/IscS	Ala/S^{2-}
0.36	0	278	302	0.92
0.72	0	234	235	1.00

[a] The cysteine desulfurase activity was assessed by analyzing for L-alanine and sulfide after anaerobic incubation with PLP, 5 mM DTT, and 500 mM L-cysteine for 2.5 h at 25 °C. [b] The detection limit for the L-alanine assay is 5 μM.

using a PLP-depleted sample of his-tagged *E. coli* IscS, a well-characterized PLP-dependent cysteine desulfurase (*49*), yielded complete reconstitution of PLP as evidenced by the extinction coefficient of bound PLP ($\epsilon_{390} = 7.5$ mM^{-1} cm^{-1}), see Figure 8.

Fontecave and co-workers reported maximal (albeit very low) levels of cysteine desulfurase activity for [4Fe−4S] BioB, with approximately six alanine and approximately six S^{2-} produced per BioB monomer after incubating with 1× PLP in the presence of 1 mM L-cysteine and 20 mM DTT for 4 h at 20 °C (*14*). However, using an assay based on L-alanine dehydrogenase (*28*), we were unable to detect L-alanine above the detection limit (5 μM) after incubating [4Fe−4S] BioB (20 or 40 μM) with 1× PLP in the presence of 500 μM L-cysteine and 5 mM DTT for 2.5 h at 25 °C, see Table 2. Sulfide was generated at the level of approximately four S^{2-} per BioB, but this was observed irrespective of the presence of PLP and the sulfide levels were never significantly greater than the amount contained in [4Fe−4S] clusters, see Table 2. Moreover, the alanine/S^{2-} ratios (<0.1) effectively rule out the possibility of cysteine desulfurase activity for these samples of [4Fe−4S] BioB. To check the effectiveness of the alanine and sulfide assays used in this work, the same protocol was used to assess cysteine desulfurase activity for his-tagged *E. coli* IscS. The results are in accord with previous assessments of IscS cysteine desulfurase activity (*23*, *49*) and indicate alanine/S^{2-} ratios close to 1.0, see Table 2.

In accord with previous activity studies of [2Fe−2S], [4Fe−4S], and [2Fe−2S]/[4Fe−4S] forms of *E. coli* BioB (*11*, *12*, *14*), none of these forms were found to be capable of more than a single turnover per BioB monomer in a well-defined anaerobic assay, see Table 1. As reported by Jarrett and co-workers (*12*), the most active form in the absence of added Fe^{2+} is [2Fe−2S]/[4Fe−4S] BioB, which undergoes almost a complete turnover based on the cluster content. [2Fe−2S] BioB exhibits negligible activity if Fe^{2+} is excluded from the reaction mixture, but the activity increases to a level close to one turnover per BioB in the presence of 1 mM $Fe^{II}(NH_4)_2(SO_4)_2$. [4Fe−4S] BioB is only capable of ∼10% of turnover in the absence of added Fe^{2+}, and this increases to ∼30% of a turnover in the presence of 1 mM $Fe^{II}(NH_4)_2(SO_4)_2$. However, in contrast to the results of Fontecave and co-workers, which reported a 5-fold increase in biotin formation for [4Fe−4S] BioB on addition of 1× PLP to the reaction mixture (*14*), the addition of 1× PLP to the reaction mixture had no significant effect on the biotin synthase activities of the [2Fe−2S], [4Fe−4S], and [2Fe−2S]/[4Fe−4S] forms of BioB investigated in this work, see Table 1.

DISCUSSION

The cofactor composition of recombinant *E. coli* BioB both in vivo and in purified samples has been the subject of much discussion and controversy since the enzyme was first purified by Sanyal and co-workers in 1994. The results presented herein are an attempt to reconcile the confusion in the literature and to establish the cofactor composition both in vivo and in as-isolated and reconstituted forms of

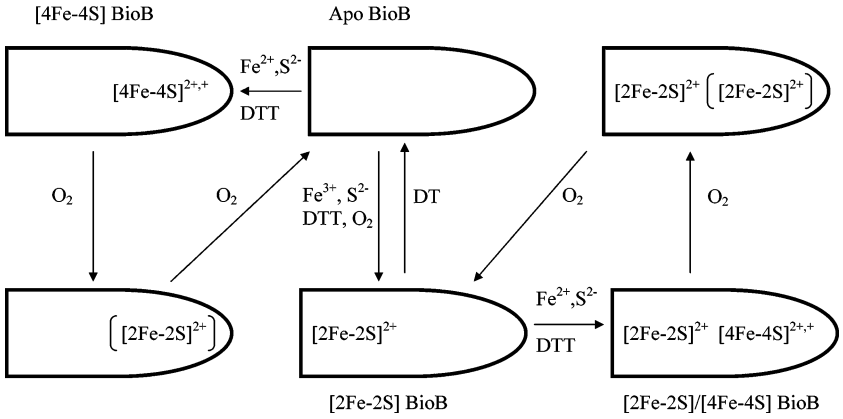

FIGURE 9: Summary of cluster-bound forms, cluster reconstitutions, and O_2-induced cluster conversions in *E. coli* BioB. An asymmetric shape is used for BioB to depict distinct cluster binding sites, and the additional parentheses indicate an intermediate $[2Fe-2S]^{2+}$ cluster that is form during O_2-induced degradation of the $[4Fe-4S]^{2+}$ cluster.

purified BioB. Perhaps most surprising is our complete failure to confirm the recent reports that BioB is a PLP-dependent enzyme with intrinsic cysteine desulfurase activity (*11*, *14*). Despite extensive assay and analytical studies using conditions similar to those reported by Fontecave and co-workers, we have been unable to find any evidence for PLP binding or for PLP-induced cysteine desulfurase or biotin synthase activity with as-isolated or reconstituted samples of purified recombinant BioB. The only significant differences between these two studies lie in our use of gel filtration rather than dialysis to remove excess PLP and in the methods used to analyze for alanine in assaying for cysteine desulfurase activity and for bound PLP. These differences are unlikely to be significant. Gel filtration is the standard method for removing excess PLP from PLP-dependent enzymes after reconstitution, and the accuracy of the analytical procedures used in this study was validated by parallel studies of IscS, a well-characterized cysteine desulfurase that binds stoichiometric PLP. Hence, we are at a loss to explain the differences between the results presented herein and those of Fontecave and co-workers, but on the basis of our results we see no reason to conclude that BioB is a PLP-dependent enzyme with cysteine desulfurase activity.

The combination of absorption, resonance Raman, and Mössbauer spectroscopies coupled with analytical studies and enzyme assays has provided a detailed understanding of the cluster composition, as well as the in vitro reconstitution products and O_2-induced cluster transformations that are possible for recombinant BioB. The results are summarized in Figure 9. In accord with the work of Jarrett and co-workers (*17*, *48*), BioB is shown to contain two distinct cluster binding sites. However, the results do not support the conclusion that each binding site can accommodate either a $[4Fe-4S]^{2+}$ or a $[2Fe-2S]^{2+}$ cluster (*17*). This conclusion was based on the ability to generate stable forms of BioB containing two $[4Fe-4S]^{2+}$ clusters per monomer or two $[2Fe-2S]^{2+}$ clusters per monomer (*17*). We have failed to confirm these results and have provided spectroscopic and analytical evidence that both forms are artifacts of analytical studies on incompletely purified reconstituted samples. Rather the results presented herein indicate that one binding site is exclusively associated with the $[2Fe-2S]^{2+}$ cluster that is present in BioB as-isolated and the other accommodates the oxygen-labile $[4Fe-4S]^{2+}$ cluster that is responsible for binding and reductive cleavage of SAM. In accord with previous results (*5*, *15*, *18*), the $[4Fe-4S]^{2+}$ cluster can be reduced to the $[4Fe-4S]^{+}$ state using dithionite or deazaflavin-mediated photochemical reduction, whereas the $[2Fe-2S]^{2+}$ cluster is slowly degraded by dithionite to yield apo BioB in the presence of an Fe chelator.

Both the $[4Fe-4S]^{2+}$ and $[2Fe-2S]^{2+}$ clusters can be reconstituted in apo BioB by incubation with Fe^{3+} or Fe^{2+} and S^{2-} in the presence of DTT, with the presence of O_2 dictating reconstitution of the $[2Fe-2S]^{2+}$ cluster and rigorously anaerobic conditions being required for reconstitution of the $[4Fe-4S]^{2+,+}$ cluster, see Figure 9. Hence the apparent discrepancy in the reconstitution products reported in the literature (*18*, *19*) can now be readily rationalized in terms of differences in the O_2 exposure during the reconstitution procedure. Anaerobic reconstitution starting with O_2-stable, as-isolated [2Fe−2S] BioB results in the formation of [2Fe−2S]/[4Fe−4S] BioB with $[2Fe-2S]^{2+}$ and $[4Fe-4S]^{2+}$ clusters in a 1:1 ratio with approximately 0.7 $[4Fe-4S]^{2+}$ and $[2Fe-2S]^{2+}$ clusters per monomer. Analogous results, albeit with near-stoichiometric $[4Fe-4S]^{2+}$ and $[2Fe-2S]^{2+}$ clusters, were first reported by Jarrett and co-workers on the basis of absorption and analytical studies (*17*), but the subsequent Mössbauer studies (*48*) would suggest a similar stoichiometry to that observed in this work. The origin of the substoichiometric amounts of each cluster is not fully understood at present. The Mössbauer evidence of substantial formation of $[^{57}Fe-4S]^{2+}$ clusters (18% of the total ^{57}Fe) during reconstitution of $[^{57}Fe-2S]$ BioB with natural abundance Fe (Figure 2e), coupled with the inability to reconstitute the $[2Fe-2S]^{2+}$ cluster under the strict anaerobic conditions of the reconstitution procedure, indicate that the substoichiometric amount of $[2Fe-2S]^{2+}$ clusters is a consequence of the lability of $[2Fe-2S]^{2+}$ cluster under reconstitution conditions. However, we currently do not have a good explanation for the observation that only ∼0.7 $[4Fe-4S]^{2+}$ clusters are assembled in reconstitutions starting from [2Fe−2S] BioB, compared to ∼1.0 $[4Fe-4S]^{2+}$ clusters in reconstitutions starting with apo BioB. Nevertheless, the analytical data and Mössbauer results can only be interpreted in terms of at least half of the protein in [2Fe−2S]/[4Fe−4S] BioB containing one $[4Fe-4S]^{2+}$ and $[2Fe-2S]^{2+}$ cluster per monomer.

The present study is particularly informative concerning the fate of the $[4Fe-4S]^{2+}$ cluster in both [4Fe−4S] and

[2Fe−2S]/[4Fe−4S] BioB during O_2-induced degradation. Resonance Raman studies show that the degradation proceeds via a $[2Fe-2S]^{2+}$ cluster intermediate that has distinctive properties compared to the $[2Fe-2S]^{2+}$ cluster in as-isolated [2Fe−2S] BioB, see Figure 9. This type of O_2-induced $[4Fe-4S]^{2+}$ cluster degradation appears to be common to most radical-SAM enzymes (*45*−*47*) and is complete in BioB after exposure to air for 10 min. However, the $[2Fe-2S]^{2+}$ cluster in the [4Fe−4S] cluster domain of BioB is less O_2-tolerant than that in some other radical SAM enzymes and is further degraded to yield a vacant [4Fe−4S] cluster domain on exposure to air for 1 h. Hence the ultimate product of exposing [2Fe−2S]/[4Fe−4S] BioB to air is [2Fe−2S] BioB. In contrast, when the [2Fe−2S] domain is vacant as in [4Fe−4S] BioB, the O_2-induced breakdown of the $[4Fe-4S]^{2+}$ cluster is followed by aerobic reconstitution of the $[2Fe-2S]^{2+}$ cluster in the [2Fe−2S] domain provided DTT is present to prevent disulfide formation, see Figure 9. It is also important to emphasize that the O_2-damaged form of [2Fe−2S]/[4Fe−4S] BioB containing two different types of $[2Fe-2S]^{2+}$ clusters does not appear to be related to the form of BioB containing two $[2Fe-2S]^{2+}$ clusters that was claimed by Jarrett and co-workers (*17*). For example, we have never observed this species in as-isolated samples of BioB or in as-isolated samples of BioB that were treated with $FeCl_3$.

The combination of resonance Raman and Mössbauer studies has also shown that SAM binds to the unique site of the $[4Fe-4S]^{2+}$ cluster in [2Fe−2S]/[4Fe−4S] BioB in the same way as previously demonstrated for [4Fe−4S] BioB (*7*). By analogy with the recent Mössbauer and electron nuclear double resonance (ENDOR) studies of the pyruvate formate-lyase activating enzyme (*50*−*52*), the mode of binding is likely to involve the amino and carboxylato groups of the methionine fragment. The observation that binding of SAM to the $[4Fe-4S]^{2+}$ cluster in [2Fe−2S]/[4Fe−4S] BioB has no effect on the spectroscopic properties of the $[2Fe-2S]^{2+}$ cluster and is unaffected by the presence of the $[2Fe-2S]^{2+}$ cluster, therefore, provides unambiguous proof for distinct [2Fe−2S] and [4Fe−4S] cluster domains with only the latter involved with binding and reductive activation of SAM. Moreover, the $[4Fe-4S]^{2+}$ cluster in [2Fe−2S]/[4Fe−4S] and [4Fe−4S] BioB was found to be essentially 100% SAM-bound using a 10-fold excess of SAM, even in the absence of DTB. This is in stark contrast to the recent results of Jarrett and co-workers (*10*), which reported negligible or weak SAM binding to the $[4Fe-4S]^{2+}$ clusters in [4Fe−4S] and [2Fe−2S]/[4Fe−4S] BioB in the absence of DTB, based on equilibrium dialysis experiments. We have no explanation for this discrepancy, but it is difficult to see how the resonance Raman and Mössbauer results can be incorrect, since they facilitate direct observation of SAM binding to the $[4Fe-4S]^{2+}$ cluster.

Our previous whole cell Mössbauer results raised the possibility that the assembly of the $[2Fe-2S]^{2+}$ cluster and the lack of assembly of the catalytically essential $[4Fe-4S]^{2+,+}$ cluster were both artifacts of overexpressing recombinant BioB under aerobic growth conditions (*24*). However, the whole cell Mössbauer studies of an anaerobically grown BioB overexpressing strain of *E. coli* that are presented in this work unambiguously demonstrate that O_2 exposure in the cell is not responsible for overexpression of recombinant BioB in an inactive form containing only the $[2Fe-2S]^{2+}$ cluster. Rather this appears to an intrinsic property of the overexpressed recombinant enzyme. However, since the recombinant form of the enzyme is expressed in an inactive form, devoid of the catalytically essential $[4Fe-4S]^{2+,+}$ cluster, under both aerobic and anaerobic growth conditions, it is still possible that the $[2Fe-2S]^{2+}$ is an artifact that is assembled in error due to absence of specific proteins or conditions that are required for assembly of the $[4Fe-4S]^{2+,+}$ cluster. In this connection, it may be significant to note that conditions have yet to be found for in vitro reconstitution of the $[2Fe-2S]^{2+}$ cluster starting with [4Fe−4S] BioB, see Figure 9. Clearly, it is now of primary importance to establish the cluster composition of native BioB at the levels expressed under normal growth conditions. Until this is accomplished, it is not possible to reach a definitive conclusion concerning the physiological relevance of the $[2Fe-2S]^{2+}$ cluster that is invariably present in as-isolated samples of recombinant BioB.

In summary, the results presented in this work do not support the proposal advanced by Fontecave and co-workers that BioB is a PLP enzyme with intrinsic cysteine desulfurase activity (*11*, *14*). They are, however, consistent with the alternative model, first advanced by Jarrett and workers (*12*, *48*), involving a functional [2Fe−2S]/[4Fe−4S] form of BioB with the $[2Fe-2S]^{2+}$ cluster as the sacrificial S donor and the $[4Fe-4S]^{2+,+}$ cluster as the site for generating the 5′-deoxyadenosyl radical via reductive cleavage of SAM. In our hands, this is the only form of BioB that is capable of a single turnover in an in vitro assay without the addition of Fe^{2+} and S^{2-}. In accord with this model, both absorption (*12*) and more recently Mössbauer (*13*) studies have shown that the $[2Fe-2S]^{2+}$ cluster is degraded during a single turnover, and labeling experiments have shown that cluster-associated S is incorporated into biotin in single turnover experiments (*36*, *53*). However, as discussed above, it is too early to speculate whether the [2Fe−2S]/[4Fe−4S] form of BioB is the catalytically relevant form that is capable of multiple turnovers in vivo. The possibility that the $[2Fe-2S]^{2+}$ cluster in [2Fe−2S]/[4Fe−4S] BioB is the immediate S donor to biotin is addressed in the following manuscript, which follows the time course of biotin production and $[2Fe-2S]^{2+}$ degradation in single turnover experiments.

REFERENCES

1. Marquet, A. (2001) Enzymology of carbon−sulfur bond formation, *Curr. Opin. Chem. Biol. 5*, 541−549.
2. Fontecave, M., Ollagnier-de-Choudens, S., and Mulliez, E. (2003) Biological radical sulfur insertion reactions, *Chem. Rev. 103*, 2149−2166.
3. Frey, P. A., and Magnusson, O. Th. (2003) *S*-Adenosylmethionine: A wolf in sheep's clothing, or a rich man's adenosylcobalamin? *Chem. Rev. 103*, 2129−2148.
4. Jarrett, J. T. (2003) The generation of 5′-deoxyadenosyl radicals by adenosylmethioine-dependent radical enzymes, *Curr. Opin. Chem. Biol. 7*, 174−182.
5. Duin, E. C., Lafferty, M. E., Crouse, B. R., Allen, R. M., Sanyal, I., Flint, D. H., and Johnson, M. K. (1997) [2Fe−2S] to [4Fe−4S] cluster conversion in *Escherichia coli* biotin synthase, *Biochemistry 36*, 11811−11820.
6. Ollagnier-de-Choudens, S., Sanakis, Y., Hewitson, K. S., Roach, P. L., Münck, E., and Fontecave, M. (2002) Reductive cleavage of *S*-adenosylmethionine by biotin synthase from *Escherichia coli*, *J. Biol. Chem. 277*, 13449−13454.
7. Cosper, M. M., Jameson, G. N. L., Davydov, R., Eidsness, M. K., Hoffman, B. M., Huynh, B. H., and Johnson, M. K. (2002)

The $[4Fe-4S]^{2+}$ cluster in reconstituted biotin synthase binds *S*-adenosylmethionine, *J. Am. Chem. Soc. 124*, 14006−14007.
8. Sofia, H. J., Chen, G., Hetzler, B. G., Reyes-Spindola, J. F., and Miller, N. E. (2001) Radical SAM, a novel protein superfamily linking unresolved steps in familiar biosynthetic pathways with radical mechanisms: functional characterization using new analysis and information visualization methods, *Nucleic Acids Res. 29*, 1097−1106.
9. Escalettes, F., Florentin, D., Tse Sum Bui, B., Lesage, D., and Marquet, A. (1999) Biotin synthase mechanism: evidence for hydrogen transfer from the substrate into deoxyadenosine, *J. Am. Chem. Soc. 121*, 3571−3578.
10. Ugulava, N. B., Frederick, K. K., and Jarrett, J. T. (2003) Control of adenosylmethionine-dependent radical generation in biotin synthase: a kinetic and thermodynamic analysis of substrate binding to active and inactive forms of BioB, *Biochemistry 42*, 2708−2719.
11. Ollagnier-de-Choudens, S., Mulliez, E., and Fontecave, M. (2002) The PLP-dependent biotin synthase from *Escherichia coli*: mechanistic studies, *FEBS Lett. 532*, 465−468.
12. Ugulava, N. B., Sacanell, C. J., and Jarrett, J. T. (2001) Spectroscopic changes during a single turnover of biotin synthase: destruction of a [2Fe−2S] cluster accompanies sulfur insertion, *Biochemistry 40*, 8352−8358.
13. Tse Sum Bui, B., Benda, R., Schünemann, V., Florentin, D., Trautwein, A. X., and Marquet, A. (2003) Fate of the $[2Fe-2S]^{2+}$ cluster of *Escherichia coli* biotin synthase during reaction: a Mössbauer characterization, *Biochemistry 42*, 8791−8798.
14. Ollagnier-de-Choudens, S., Mulliez, E., Hewitson, K. S., and Fontecave, M. (2002) Biotin synthase is a pyridoxal phosphate-dependent cysteine desulfurase, *Biochemistry 41*, 9145−9152.
15. Sanyal, I., Cohen, G., and Flint, D. H. (1994) Biotin synthase: purification, characterization as a [2Fe−2S] cluster protein, and in vitro activity of the *Escherichia coli bioB* gene product, *Biochemistry 33*, 3625−3631.
16. Picciocchi, A., Douce, R., and Alban, C. (2001) Biochemical characterization of the Arabidopsis biotin synthase reaction. The importance of mitochondria in biotin synthesis, *Plant Physiol. 127*, 1224−1233.
17. Ugulava, N. B., Gibney, B. R., and Jarrett, J. T. (2001) Biotin synthase contains two distinct iron−sulfur cluster binding sites: chemical and spectroelectrochemical analysis of iron−sulfur cluster interconversions, *Biochemistry 40*, 8343−8351.
18. Ollagnier-de-Choudens, S., Sanakis, Y., Hewitson, K. S., Roach, P., Baldwin, J. E., Münck, E., and Fontecave, M. (2000) Iron−sulfur center of biotin synthase and lipoate synthase, *Biochemistry 39*, 4165−4173.
19. Tse Sum Bui, B., Florentin, D., Marquet, A., Benda, R., and Trautwein, A. X. (1999) Mössbauer studies of *Escherichia coli* biotin synthase: evidence for reversible interconversion between $[2Fe-2S]^{+}$ and $[4Fe-4S]^{2+}$ clusters, *FEBS Lett. 459*, 411−414.
20. Hewitson, K. S., Baldwin, J. E., Shaw, N. M., and Roach, P. L. (2000) Mutagenesis of the proposed iron−sulfur cluster binding ligands in *Escherichia coli* biotin synthase, *FEBS Lett. 466*, 372−376.
21. Hewitson, K. S., Ollagnier-de-Choudens, S., Sanakis, Y., Shaw, N. M., Baldwin, J. E., Münck, E., Roach, P. L., and Fontecave, M. (2002) The iron−sulfur center of biotin synthase: site-directed mutants, *J. Biol. Inorg. Chem. 7*, 83−93.
22. Zheng, L., White, R. H., Cash, V. L., Jack, R. F., and Dean, D. R. (1993) Cysteine desulfurase activity indicates a role for NIFS in metallocluster biosynthesis, *Proc. Natl. Acad. Sci. U.S.A. 90*, 2754−2758.
23. Mihara, H., and Esaki, N. (2002) Bacterial cysteine desulfurases: their function and mechanisms, *Appl. Microbiol. Biotechnol. 60*, 12−23.
24. Cosper, M. M., Jameson, G. N. L., Eidsness, M. K., Huynh, B. H., and Johnson, M. K. (2002) Recombinant *Escherichia coli* biotin synthase is a $[2Fe-2S]^{2+}$ protein in whole cells, *FEBS Lett. 529*, 332−336.
25. Benda, R., Tse Sum Bui, B., Schünemann, V., Florentin, D., Marquet, A., and Trautwein, A. X. (2002) Iron−sulfur clusters of biotin synthase in vivo: a Mössbauer study, *Biochemistry 41*, 15000−15006.
26. Tabor, S. (1990) Expression using the T7 RNA polymerase/promotor system, in *Current Protocols in Molecular Biology* (Ausubel, F. A., Brent, R., Kingston, R. E., Moore, D. D., Seidman, J. G., Smith, J. A., and Sthuhl, K., Eds.) pp 16.2.1−16.2.11, Greene Publishing and Wiley-Interscience, New York.
27. Harwood, C. R., and Cutting, S. M. (1990) *Modern Microbiological Methods: Molecular Biology Methods for Bacillus*, Wiley and Sons, Chichester, U.K.
28. Yoshida, A., and Freese, E. (1970) L-Alanine dehydrogenase (*Bacillus subtilis*), *Methods Enzymol. 17a*, 176−181.
29. Siegel, L. M. (1965) A direct microdetermination for sulfide, *Anal. Biochem. 11*, 126−132.
30. Fish, W. W. (1988) Rapid colorimetric micromethod for the quantitation of complexed iron in biological samples, *Methods Enzymol. 158*, 357−364.
31. Bates, C. J., Pentieva, K. D., Matthews, N., and Macdonald, A. (1999) A simple, sensitive and reproducible assay for pyridoxal 5′-phosphate and 4-pyridoxic acid in human plasma, *Clin. Chim. Acta 280*, 101−111.
32. Drozdzewski, P. M., and Johnson, M. K. (1988) A simple anaerobic cell for low-temperature Raman spectroscopy, *Appl. Spectrosc. 42*, 1575−1577.
33. Ravi, N., Bollinger, J. M., Huynh, B. H., Edmondson, D. E., and Stubbe, J. (1994) Mechanism of assembly of the tyrosyl radical-diiron(III) cofactor of *E. coli* ribonucleotide reductase. 1. Mössbauer characterization of the diferric radical precusor, *J. Am. Chem. Soc. 116*, 8007−8014.
34. Tanaka, M., Izumi, Y., and Yamada, H. (1987) Biotin assay using lyophilized and glycerol-suspended cultures, *J. Microbiol. Methods 6*, 237−246.
35. Tse Sum Bui, B., and Marquet, A. (1997) Biotin synthase of *Bacillus sphaericus*, *Methods Enzymol. 279*, 357−362.
36. Tse Sum Bui, B., Florentin, D., Fournier, F., Ploux, O., Méjean, A., and Marquet, A. (1998) Biotin synthase mechanism: on the origin of sulphur, *FEBS Lett. 440*, 226−230.
37. Spiro, T. G., Hare, J., Yachandra, V., Gewirth, A., Johnson, M. K., and Remsen, E. (1982) Resonance Raman spectra of iron−sulfur proteins and analogues, in *Iron−sulfur proteins* (Spiro, T. G., Ed.) pp 407−423, Wiley-Interscience, New York.
38. Spiro, T. G., Czernuszewicz, R. S., and Han, S. (1988) Iron−sulfur proteins and analogue complexes, in *Resonance Raman spectra of heme and metalloproteins* (Spiro, T. G., Ed.) pp 523−554, John Wiley & Sons, New York.
39. Fu, W., Morgan, T. V., Mortenson, L. E., and Johnson, M. K. (1991) Resonance Raman studies of the [4Fe−4S] to [2Fe−2S] cluster conversion in the iron protein of nitrogenase, *FEBS Lett. 284*, 165−168.
40. Fu, W., Drozdzewski, P. M., Adams, M. W. W., Morgan, T. V., Mortenson, L. E., LeGall, J., Peck, H. D., Jr., DerVartanian, D. V., and Johnson, M. K. (1993) Resonance Raman studies of iron−hydrogenases, *Biochemistry 32*, 4813−4819.
41. Tong, W.-H., Jameson, G. N. L., Huynh, B. H., and Rouault, T. A. (2003) Subcellular compartmentalization of human Nfu, an iron−sulfur cluster scaffold protein and its ability to assemble a [4Fe−4S] cluster, *Proc. Natl. Acad. Sci. U.S.A. 100*, 9762−9767.
42. Trautwein, A. X., Bominaar, E. L., and Winkler, H. (1991) Iron-containing proteins and related analogues. Complementary Mössbauer, EPR and magnetic susceptibility studies, *Struct. Bonding 78*, 1−95.
43. Krebs, C., Agar, J. N., Smith, A. D., Frazzon, J., Dean, D. R., Huynh, B. H., and Johnson, M. K. (2001) IscA, an alternative scaffold for Fe−S cluster biosynthesis, *Biochemistry 40*, 14069−14080.
44. Johnson, M. K., Staples, C. R., Duin, E. C., Lafferty, M. E., and Duderstadt, R. E. (1998) Novel roles for Fe−S cluster in stabilizing or generating radical intermediates, *Pure Appl. Chem. 70*, 939−946.
45. Ollagnier, S., Meier, C., Mulliez, E., Gaillard, J., Schuenemann, V., Trautwein, A. X., Mattioli, T., Lutz, M., and Fontecave, M. (1999) Assembly of 2Fe−2S and 4Fe−4S clusters in the anaerobic ribonucleotide reductase from *Escherichia coli*, *J. Am. Chem. Soc. 121*, 6344−6350.
46. Broderick, J. B., Duderstadt, R. E., Fernandez, D. C., Wojtuszewski, K., Henshaw, T. F., and Johnson, M. K. (1997) Pyruvate formate-lyase activating enzyme is an iron−sulfur protein, *J. Am. Chem. Soc. 119*, 7396−7397.
47. Pierrel, F., Hernandez, H., Johnson, M. K., Fontecave, M., and Atta, M. (2003) MiaB protein from *Thermotoga maritime*: characterization of an extremely thermophilic tRNA-methylthiotransferase, *J. Biol. Chem. 278*, 29515−29524.
48. Ugulava, N. B., Surerus, K. K., and Jarrett, J. T. (2002) Evidence from Mössbauer spectroscopy for distinct $[2Fe-2S]^{2+}$ and $[4Fe-4S]^{2+}$ cluster binding sites in biotin synthase from *Escherichia coli*, *J. Am. Chem. Soc. 124*, 9050−9051.

49. Flint, D. H. (1996) *Escherichia coli* contains a protein that is homologous in function and N-terminal sequence to the protein encoded by the NIFS gene of *Azotobacter vinelandii* and that can participate in the synthesis of the Fe−S cluster of dihyroxy-acid dehydratase, *J. Biol. Chem. 271*, 16068−16074.
50. Krebs, C., Broderick, W. E., Henshaw, T. F., Broderick, J. B., and Huynh, B. H. (2002) Coordination of adenosylmethionine to a unique iron site of the [4Fe−4S] cluster of pyruvate formate-lyase activating enzyme: a Mössbauer spectroscopic study, *J. Am. Chem. Soc. 124*, 912−913.
51. Walsby, C. J., Hong, W., Broderick, W. E., Cheek, J., Ortillo, D., Broderick, J. B., and Hoffman, B. M. (2002) Electron−nuclear double resonance spectroscopic evidence that *S*-adenosylmethionine binds in contact with the catalytically active $[4Fe-4S]^{+}$ cluster in pyruvate formate-lyase activating enzyme, *J. Am. Chem. Soc. 124*, 3143−3151.
52. Walsby, C. J., Ortillo, D., Broderick, W. E., Broderick, J. B., and Hoffman, B. M. (2002) An anchoring role for FeS clusters: chelation of the amino acid moiety of *S*-adenosylmethionine to the unique iron site of the [4Fe−4S] cluster of pyruvate formate-lyase activating enzyme, *J. Am. Chem. Soc. 124*, 11270−11271.
53. Gibson, K. J., Pelletier, D. A., and Turner, I. M., Sr. (1999) Transfer of sulfur to biotin from biotin synthase (bioB protein), *Biochem. Biophys. Res. Commun. 254*, 632−635.

BI0356653